

## Energetic Salts of Low-Symmetry Methylated 5-Aminotetrazoles

Thomas M. Klapötke,<sup>\*[a]</sup> Carles Miró Sabaté,<sup>[a]</sup> Alexander Penger,<sup>[a]</sup> Magdalena Rusan,<sup>[a]</sup> and Jan M. Welch<sup>[a]</sup>**Keywords:** Density functional calculations / Energetic materials / Heterocycles / Secondary interactions

Ionic salts containing the novel 5-amino-2-methyl- and 5-amino-1,3-dimethyltetrazolium cations with energetic anions (perchlorate, nitrate, azide and dinitramide) have been synthesized in high yields and purities and fully characterized. A full structural description by spectroscopic methods (vibrational and <sup>15</sup>N NMR spectroscopy) and X-ray analysis is given. Unexpectedly, salts based on the asymmetric 5-amino-1,3-dimethyltetrazolium cation have higher densities than analogue compounds containing the isomeric 5-amino-1,4-

dimethyltetrazolium cation, regardless of the lower symmetry of the former. This can be attributed to secondary interactions between the cation and anion and is reflected in the higher detonation parameters of the new compounds, which represent a new class of nitrogen-rich, high-performing materials with low sensitivity and good potential for energetic applications.

(© Wiley-VCH Verlag GmbH & Co. KGaA, 69451 Weinheim, Germany, 2009)

## Introduction

One of the general goals of modern energetic materials development is the synthesis of materials with acceptable performances and very low sensitivities to physical stimuli. Unfortunately, the performance and sensitivity properties of an explosive material are linked both to each other and to the general physical and chemical properties of that material. To counteract the correlation of high performance (high detonation pressure and velocity) with high sensitivity to impact, friction and shock systems, compounds such as 1,1-diamino-2,2-dinitroethene (FOX-7)<sup>[1]</sup> or 1,3,5-triamino-2,4,6-trinitrobenzene,<sup>[2]</sup> which form extensive hydrogen-bonding networks in the solid state, are the state of the art. Hydrogen-bonding networks (especially between amino and nitro groups) like those formed in FOX-7 and TATB help to stabilize the material substantially without dramatically reducing energetic performance.

On the other hand, ionic energetic materials based on azoles (in particular aminotetrazoles) and other nitrogen-rich compounds are also known to form strong hydrogen-bonding networks and thus show remarkable stability and considerable insensitivity to physical stimuli as well as good performance.<sup>[3–7]</sup> With these properties in mind, aminotetrazole-based compounds (Figure 1) have long been of interest as potential energetic materials. We recently studied a family of simple energetic salts based on the major mono-

methylation product of 5-amino-1*H*-tetrazole (**1**), 5-amino-1-methyltetrazole (**4**). In that study, **4** was protonated with strong mineral acids (perchloric and nitric acid) and also quaternized with methyl iodide to yield, after metathesis reactions, a series of salts based on 5-imino-1,4-dimethyltetrazole (1,4DMIT)<sup>[8]</sup>

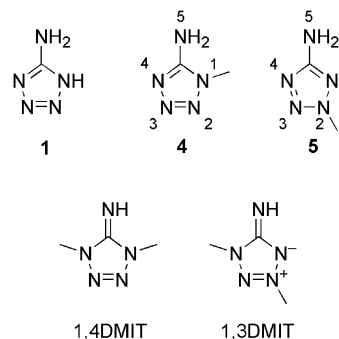


Figure 1. Structural formula of the 5-aminotetrazoles: 5-amino-1*H*-tetrazole (**1**), 5-amino-1-methyltetrazole (**4**), 5-amino-2-methyltetrazole (**5**), 5-imino-1,4-dimethyltetrazole (1,4DMIT) and 5-imino-1,3-dimethyltetrazole (1,3DMIT).

Initially, we ignored the salts of 5-amino-2-methyltetrazole (**5**) and those of 5-imino-1,3-dimethyltetrazole (1,3DMIT) because **5** is only formed as a minor product (10–20% depending on conditions) of the above-mentioned methylation of **1**.<sup>[9]</sup> However, given the current interest in ionic-liquid-based energetic systems and the low symmetry of the cation of 1,3DMIT (an important criteria for potential ionic liquid formation) we have investigated a new method for the synthesis of **5** as well as the structure and properties of ionic energetic salts based on **5** and 1,3DMIT

[a] Department of Chemistry and Biochemistry, Energetic Materials Research, Ludwig-Maximilian University, Butenandstr. 5–13, 81377, Munich, Germany  
Fax: +49-89-2180-77492

E-mail: tmk@cup.uni-muenchen.de

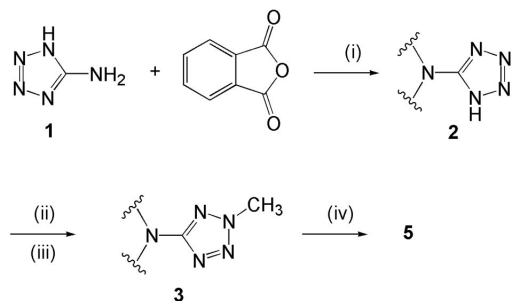
Supporting information for this article is available on the WWW under <http://www.eurjic.org> or from the author.

in the hope of developing a second family of new materials of low sensitivity and potentially new liquid ionic energetic materials.

## Results and Discussion

### Synthesis

As mentioned in the previous section, **5** can be obtained by methylation of the sodium salt of 5-aminotetrazole (**1**) with dimethyl sulfate as the minor isomer together with **4** (major isomer), as described in the literature.<sup>[9]</sup> We present here a new method involving the deactivation of the amino group in **1** by protection with phthalic acid anhydride to form *N*-(1*H*-tetrazol-5-yl)phthalimide (**2**).<sup>[10]</sup> Compound **2** can be selectively methylated with methyl iodide or dimethyl sulfate to form exclusively *N*-(2-methyltetrazol-5-yl)phthalimide (**3**) and deprotection of **3** gives **5** in an improved overall yield of around 47% (Scheme 1). Compound **5** (obtained by either one of the two methods) can react with strong



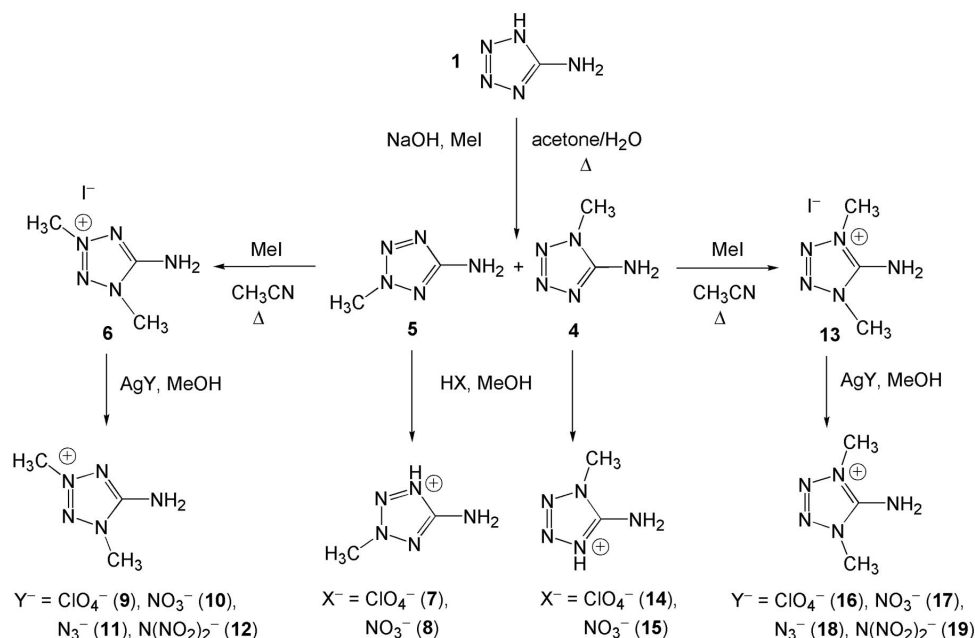
Scheme 1. Improved synthesis of 5-amino-2-methyltetrazole (**5**). Reagents and conditions: (i)  $\text{CH}_3\text{CO}_2\text{H}$ ,  $\Delta$ ; (ii)  $\text{NaHCO}_3$ ,  $\text{H}_2\text{O}$ , (iii)  $\text{MeI}$ , acetone,  $\Delta$ ; (iv)  $\text{N}_2\text{H}_4 \cdot \text{H}_2\text{O}$ , ethanol,  $\Delta$ .

acids (either perchloric or nitric acid) to generate the corresponding energetic perchlorate **7** and nitrate salts **8**. Similarly to our previous work on the energetic salts of **4**,<sup>[8]</sup> every attempt to generate the energetically interesting salt was in vain.<sup>[8,11]</sup> On the other hand, methylation of **5** with methyl iodide using acetonitrile as the solvent resulted in the regioselective methylation of **5**, yielding the iodide salt **6**,<sup>[12]</sup> which was used as the starting material for the synthesis of the energetic salts of 1,3DMIT with perchlorate **9**, nitrate **10**, azide **11** and dinitramide **12** anions. The general method (illustrated in Scheme 2) involves a metathesis reaction of iodide **6** and a suitable “energetic anion transfer reagent”, generally a silver salt (see Expt. Sect.).

Most of the energetic compounds were obtained in excellent yields and purities and crystalline materials formed when diffusing diethyl ether into a saturated alcoholic solution of the salts. Lastly, all energetic salts described herein are readily soluble in polar solvents such as methanol, ethanol, water, DMF, DMSO or acetonitrile and insoluble or little soluble in less polar or apolar solvents such as THF, DCM, diethyl ether or pentane.

### Vibrational Spectroscopy

Compounds **2**, **3** and the salts of **5** and 1,3DMIT, generated as described above, were qualitatively identified by vibrational spectroscopy (IR and Raman). A discussion of the spectra of the starting materials **2** and **3** is beyond the scope of this section. The spectra (both IR and Raman) of **5** are in perfect agreement with those reported in the literature.<sup>[13]</sup> The spectrum of each compound showed characteristic bands of the relevant energetic anion (nitrate, perchlorate, azide or dinitramide) and a set of bands corresponding to the cation. The nitrate anion,  $\text{NO}_3^-$ , shows a



Scheme 2. Synthesis of the energetic salts of 5-amino-2-methyltetrazole (**5**) and 5-imino-1,3-dimethyltetrazole (1,3DMIT).

strong (or very strong) IR absorption centred at  $1384\text{ cm}^{-1}$  (both **8** and **10**; Figure 2) and a sharp band at around  $1045\text{ cm}^{-1}$  in the Raman spectrum.<sup>[14]</sup> Compound **8** shows a broad IR signal of medium intensity with a maxima at  $1308\text{ cm}^{-1}$ , which is masked by the absorptions of the cation in salt **10**. Salts of the perchlorate anion,  $\text{ClO}_4^-$ , show a strong or very strong broad stretch with a maximum at around  $1090\text{ cm}^{-1}$  in the IR spectra and strong, sharp bands at around  $930$  and  $465\text{ cm}^{-1}$  in the Raman spectra.<sup>[15]</sup> The asymmetric stretch of the anion in compound **11** is observed as a strong absorption at  $2042\text{ cm}^{-1}$ , whereas the symmetric stretch is weak in intensity and found at  $1297\text{ cm}^{-1}$  in the IR spectrum. In the Raman spectrum only the symmetric stretch is observed as a strong band at  $1301\text{ cm}^{-1}$ , as is usual for ionic azides.<sup>[16]</sup> In contrast to the azide salt of 1,4DMIT, the absence of the asymmetric stretch in the Raman spectrum of azide salt **11** indicates that only weak interactions between the cation and anion are present. The dinitramide anion,  $\text{N}(\text{NO}_2)_2^-$ , in salt **12** has medium-to-very strong absorptions at  $1515$ ,  $1430$ ,  $1384$ ,  $1186$  and  $1011\text{ cm}^{-1}$  in the IR spectrum and strong bands in the Raman spectrum at  $1324$  and  $825\text{ cm}^{-1}$ .<sup>[17]</sup> Bands corresponding to the cation can be assigned as follows:  $3500\text{--}3100$  [ $\nu(\text{N-H})$ ],  $3000\text{--}2850$  [ $\nu(\text{C-H})$ ], ca.  $1660$  [ $\nu(\text{C5=N5}) + \delta(\text{N5H}_2)$ ],  $1550\text{--}1350$  [ $\nu(\text{tetrazole ring})$ ,  $\delta_{\text{as}}(\text{CH}_3)$ ,  $\delta(\text{N4-H})$ ], ca.  $1380$  [ $\delta(\text{CH}_3)$ ],  $1350\text{--}700$  [ $\nu(\text{N1-C1-N4})$ ,  $\nu(\text{N-N})$ ,  $\gamma(\text{CN})$ ,  $\delta(\text{tetrazole ring})$ ] and  $<700\text{ cm}^{-1}$  [ $\delta$  out-of-plane bend (N-H),  $\omega(\text{N5H}_2)$ ].<sup>[8,18]</sup>

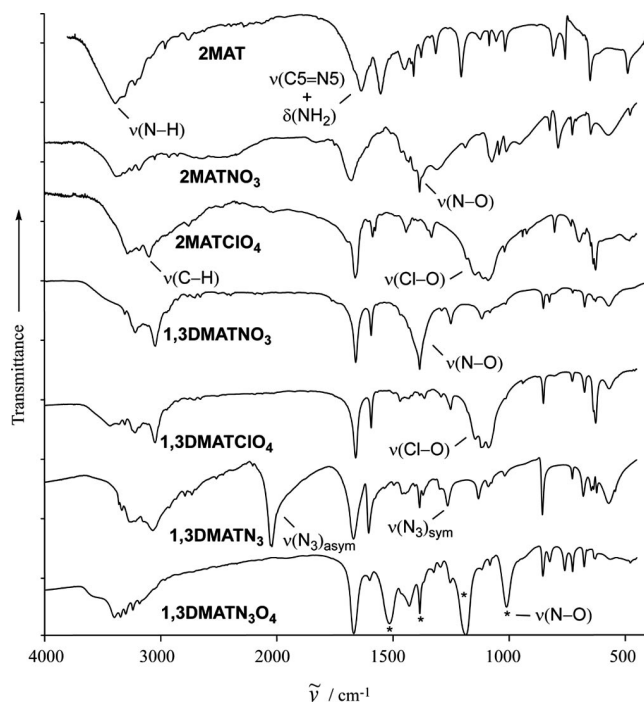


Figure 2. Panel plot of the IR spectra of the energetic salts of 5-amino-2-methyltetrazole (**5**) and 5-imino-1,3-dimethyltetrazole (1,3DMIT). 1,3DMAT = 5-amino-1,3-dimethyltetrazol-3-ium.

In addition to allowing a quick, qualitative identification of the materials, vibrational spectroscopy also provides an insight into their structural features, specifically of the cat-

ion and hydrogen-bonding found in each material studied. Of particular interest are the vibrations corresponding to N-H stretches and deformations and the coupled C5=N5 stretching and N5H<sub>2</sub> deformation modes. These bands are sensitive indicators of hydrogen-bond strength and the geometry of the exocyclic amino group. The neutral parent compounds **4** and **5** show slightly different energies for the above-mentioned vibrations. The N5-H stretching modes are observed at slightly higher energies for **5** and the C5=N5 stretching and N5H<sub>2</sub> deformation vibrations at slightly lower energies, which indicates weaker hydrogen-bonding and a weaker (longer) C5=N5 bond in **5** compared with in **4**. This relationship is also observed in the N5-H stretches and deformations and the coupled C5=N5 stretching and N5H<sub>2</sub> deformation modes in the ionic species based on 1,4DMIT and 1,3DMIT, which points to less C5=N5 double bond character in the cations based on **5** and weaker hydrogen-bonding interactions between the cations and anions in the salts of **5** and 1,3DMIT as opposed to the stronger interactions observed for the salts of **4** and 1,4DMIT.

Within the series of salts based on **4** and 1,4DMIT, on the basis of IR spectroscopy, we observed a trend in hydrogen-bond strength that is dependent on the anion used. In the case of the compounds in the current study, the nitrate salt **8** shows stronger hydrogen-bonding (the presence of a broad absorption centred at ca.  $2400\text{ cm}^{-1}$ ) than the perchlorate salt **7** (no absorptions are observed in the range  $2800\text{--}1800\text{ cm}^{-1}$ ), as is expected and as was the case for salts based on **4**. However, in contrast to the IR spectra of the salts based on 1,4DMIT, the spectra of the salts based on 1,3DMIT (compounds **6–12**) show no such trend. Compounds **6–12** all have, aside from bands attributed to the anions, nearly identical IR and Raman spectra. This indicates not only that hydrogen-bonding is not particularly pronounced in any one compound in this series, but also that the cations are expected to be very nearly structurally identical (for further details see the Molecular Structures section). The relatively weak hydrogen-bonding in the salts of 1,3DMIT, as compared to salts of 1,4DMIT, may be clarified by differences in cation acidity.

### NMR Spectroscopy

Each compound studied in this work was characterized by multinuclear (<sup>1</sup>H, <sup>13</sup>C, <sup>15</sup>N and when applicable <sup>35</sup>Cl) NMR spectroscopy. The chemical shifts recorded for all nuclei as well as the <sup>1</sup>J, <sup>2</sup>J and <sup>3</sup>J (<sup>1</sup>H-<sup>15</sup>N) coupling constants are reported in the Exptl. Sect. In the case of **5**, all recorded signals and <sup>1</sup>J(<sup>1</sup>H-<sup>15</sup>N) couplings are in very good agreement with previous studies by our group and the <sup>1</sup>H and <sup>13</sup>C resonances are observed as expected.<sup>[8,11,19]</sup>

Once again, the discussion of the NMR spectroscopic data for the starting materials **2** and **3** is beyond the scope of this paper. Figures S1 and S2 in the Supporting Information show a section of the <sup>1</sup>H NMR spectra for the AA'BB' spin system region of the two compounds for illus-

Table 1.  $^{15}\text{N}$  and  $^{13}\text{C}$  NMR chemical shifts and protonation (PIS)/methylation (MIS)-induced shifts in  $[\text{D}_6]\text{DMSO}$ .<sup>[a]</sup>

	$\delta$ [ppm] ( $\Delta\delta$ [ppm])					
	N1 (N4)	N2 (N3)	N3 (N2)	N4 (N1)	N5	C <sub>ring</sub>
<b>4</b> <sup>[b]</sup>	-185	-23.2	2.2	-92.7	-338.2	156.4
<b>13</b> <sup>[b]</sup>	-182.9 (2.1)	-29.9 (-6.7)	-29.9 (-32.1)	-182.9 (-90.2)	-318 (20.2)	149.1
<b>14</b> <sup>[b]</sup>	-183.8 (1.2)	-24.3 (-1.1)	-17.4 (-19.6)	-139.1 (-46.4)	-329.5 (8.7)	155.2
<b>15</b> <sup>[b]</sup>	-184.0 (1.0)	-24 (-0.8)	-13.5 (-15.7)	-129.7 (-37)	-331.4 (6.8)	153.6
<b>16</b> <sup>[b]</sup>	-182.9 (2.1)	-29.5 (-6.3)	-29.5 (-31.7)	-182.9 (-90.2)	-320 (18.2)	148.5
<b>17</b> <sup>[b]</sup>	-182.8 (2.2)	-29.5 (-6.3)	-29.5 (-31.7)	-182.8 (-90.1)	-320.4 (17.8)	148.9
<b>18</b> <sup>[b]</sup>	-185.8 (-0.8)	-30.7 (-7.5)	-30.7 (-32.9)	-185.8 (-93.1)	-307.2 (31.0)	148.8
<b>19</b> <sup>[b]</sup>	-182.7 (2.3)	-29.4 (-6.2)	-29.4 (-31.6)	-182.7 (-90.0)	-320.1 (18.1)	148.5
<b>5</b>	-115.6	-115.7	-6.5	-83.3	-339.7	167.7
<b>6</b>	-109.0 (6.6)	-111.3 (4.4)	-31.8 (-25.3)	-180.6 (-97.3)	-324.4 (15.3)	157.8
<b>7</b>	-113.4 (2.2)	-114.2 (1.5)	-8.8 (-2.3)	-90.0 (-6.7)	-340.1 (-0.4)	166.8
<b>8</b>	-114.4 (1.2)	-114.9 (0.8)	-6.9 (-0.4)	-84.4 (-1.1)	-339.5 (0.2)	167.2
<b>9</b>	-109.3 (6.3)	-111.3 (4.4)	-31.4 (-24.9)	-180.3 (-97.0)	-327.2 (12.5)	158.1
<b>10</b>	-109.6 (6.0)	-111.1 (4.6)	-32.6 (-26.1)	-181.2 (-97.9)	-326.0 (13.7)	158.6
<b>11</b>	-113.2 (2.4)	-113.4 (2.3)	-33.1 (-26.6)	-189.0 (-105.7)	-327.6 (12.1)	158.1
<b>12</b>	-109.4 (6.2)	-111.2 (4.5)	-33.3 (-26.8)	-181.1 (-97.8)	-326.8 (12.9)	158.6

[a] PIS and MIS shifts are given in parentheses. [b] From ref.<sup>[8]</sup>: **13**: 5-amino-1,4-dimethyltetrazolium iodide; **14**: 5-amino-1-methyltetrazolium perchlorate; **15**: 5-amino-1-methyltetrazolium nitrate; **16**: 5-amino-1,4-dimethyltetrazolium perchlorate; **17**: 5-amino-1,4-dimethyltetrazolium nitrate; **18**: 5-amino-1,4-dimethyltetrazolium azide; **19**: 5-amino-1,4-dimethyltetrazolium dinitramide.

tration purposes. The  $^1\text{H}$  NMR spectra of all the salts measured in  $[\text{D}_6]\text{DMSO}$  show two or three resonances for the protons in the cation of **5** and 1,3DMIT, respectively. The sharp peaks of the methyl group protons occur at  $\delta \approx 4.0$  ppm (salts of **5**) and at  $\delta \approx 4.2$  and 3.9 ppm (salts of 1,3DMIT). A broadened peak corresponding to the protons of the amino group occurs at above  $\delta = 8.0$  ppm for all compounds. In the  $^{13}\text{C}$  NMR spectra, the tetrazole carbon signal of the cation is found at  $\delta \approx 167.0$  ppm for the salts of **5** and is shifted to high field in the salts of 1,3DMIT ( $\delta \approx 158.3$  ppm). Similarly to observations in the  $^1\text{H}$  NMR spectra, the signals corresponding to the methyl groups in compounds **7** and **8** ( $\delta \approx 40.0$  ppm) are found at high field with respect to the N3-CH<sub>3</sub> carbon atom resonance ( $\delta \approx 43.0$  ppm) and to low field compared with the N1-CH<sub>3</sub> carbon atom resonance ( $\delta \approx 34.4$  ppm). In the  $^{15}\text{N}$  NMR spectra of all compounds (Table 1), five resonances (all in the negative range) can be observed as a consequence of low symmetry, which may be assigned to the cations of **5** and 1,3DMIT (see Figure 3 and the Exptl. Sect.). In general, every nitrogen atom in the cation of 1,3DMIT shows coupling to protons. The amino group nitrogen atom couples at one bond to its protons with  $^1J \approx 90.0$  Hz. The nitrogen atoms N1 and N3 couple at two bonds and N2 and N4 at three bonds to the hydrogen atoms of the methyl groups with coupling constants that vary between around 1.9 and 2.7 Hz. In addition, resonances corresponding to the anion are also observed. Compounds **4** and **8** show a peak at  $\delta \approx -5$  ppm in the  $^{15}\text{N}$  NMR spectra corresponding to the nitrogen atom of the nitrate anion. In the  $^{15}\text{N}$  NMR spectra of the azide salt **11** two further resonances at  $\delta \approx -135$  and  $-285$  ppm can be observed corresponding to the nitrogen atoms of the azide anion, similar to the  $^{14}\text{N}$  NMR resonances. The dinitramide salt **12** shows additional signals at  $\delta \approx -11$  and  $-57$  ppm corresponding to the nitrogen atoms of the nitro groups and the bridging nitrogen atom in the

anion, respectively. Lastly, the chlorine atom of the perchlorate anion of salts **7** and **9** shows a resonance at  $\delta \approx 1.0$  ppm in the  $^{35}\text{Cl}$  NMR spectra of the compounds.

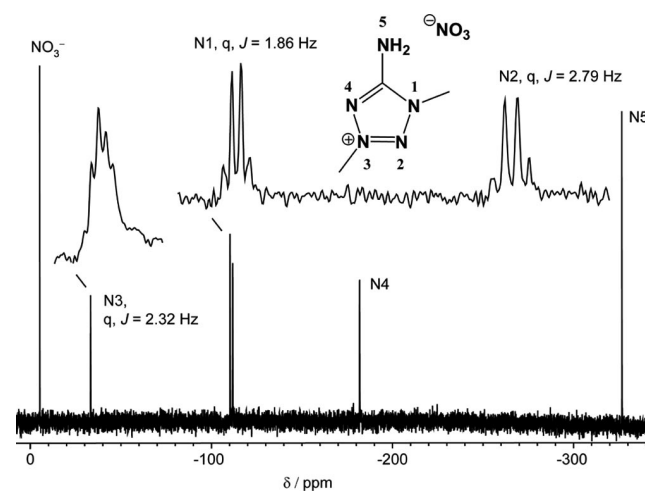


Figure 3.  $^{15}\text{N}$  NMR spectrum of the 5-amino-1,3-dimethyltetrazolium cation in compound **10**, recorded in  $[\text{D}_6]\text{DMSO}$ .

In addition to providing a quick method to uniquely identify the compounds synthesized and help with the assignment of the resonances, protonation- and methylation-induced shifts [**7** and **8** (PIS) and **6–12** (MIS), respectively, calculated as the difference in  $^{15}\text{N}$  NMR shifts between analogous nitrogen signals arising from neutral **5** and the salts of **5** and 1,3DMIT]<sup>[11]</sup> can be used to derive information about the structure in solution and hydrogen-bonding (interionic interactions).<sup>[8,11,20]</sup> As was the case for the nitrate and perchlorate salts of **4**, the PIS data for **7** and **8** show the most significant shifts occurring at N4, which indicates that protonation in solution occurs primarily at N4. However, the shifts themselves are quite small in comparison to those observed for other ring-protonated hetero-

cyclic salts, which seems to indicate that in DMSO solution **7** and **8** exist primarily as **5** and nitric and perchloric acid, respectively. The dissociation of the salts in solution seems to corroborate the IR spectroscopic observation that interionic interactions are weaker for the salts of **5** than they are for the salts of **4**. The N1 resonance shows an MIS of approximately  $-97$  ppm compared with N4 of **5**. The observed resonances and MIS values observed and calculated for all the salts of 1,3DMIT, except for **11**, are all very nearly equal within the tolerances of the measurement. The salt **11** shows the strongest cation–anion interactions and thus the least positive (or most negative) MIS values, as would be expected, because the resonances observed for the cation in **11** should tend towards the values observed for 1,3DMIT. The remaining MIS data simply indicate a great deal of similarity in the strength of the interaction between the cation and the different anions in solution.

### Molecular Structures

The structures of all the salts of **5** and 1,3DMIT and that of the neutral parent compound **5** were determined by X-ray diffraction. Crystals were grown as summarized in the Exptl. Sect. Crystallographic data and structure determination details are presented in the Supporting Information (Table S1). Selected interatomic distances and angles are shown in Table 2 and hydrogen-bond parameters are tabulated in Table 3. The X-ray crystallographic data for **8** were collected with an Enraf–Nonius Kappa CCD diffractometer. Data sets for the other compounds were collected with an Oxford Diffraction Xcalibur 3 diffractometer equipped with a CCD detector. All data were collected by using graphite-monochromated Mo- $K_{\alpha}$  radiation ( $\lambda = 0.71073$  Å). No absorption corrections were applied to the data set collected for **8**. A multiscan numerical absorption correction was applied to data collected for the remainder of the compounds in this study using the ABSPACK<sup>[21]</sup> software supplied by Oxford Diffraction. All structures

were solved by direct methods (SIR92)<sup>[22]</sup> and refined by means of full-matrix least-squares procedures using SHELXL-97<sup>[23]</sup> implemented in the WingGX software package<sup>[24]</sup> and the structures were finally checked using PLATON.<sup>[25]</sup> All non-hydrogen atoms were refined anisotropically. For all compounds all hydrogen atoms were located from difference Fourier electron-density maps and refined isotropically.

CCDC-704518 (for **5**), -704519 (for **7**), -704520 (for **8**), -704521 (for **9**), -704522 (for **10**), -704523 (for **11**) and -704524 (for **12**) contain the supplementary crystallographic data for this paper. This data can be obtained free of charge from The Cambridge Crystallographic Data Centre via [www.ccdc.cam.ac.uk/data\\_request/cif](http://www.ccdc.cam.ac.uk/data_request/cif).

The crystal structure of neutral **5** was first determined by Bryden in 1956.<sup>[26]</sup> Therefore, only the details of the improved structure measured here that are of interest will be discussed. The bond lengths in the tetrazole ring for the rest of the materials vary between around 1.28 and 1.35 Å (Table 2) and lie in the range between N–N single bonds (1.45 Å) and N=N double bonds (1.25 Å). Also the ring C–N distances are between around 1.31 and 1.36 Å, within the range expected for C–N single and C=N double bonds.<sup>[27]</sup>

Compound **5** crystallizes in layers, which are perfectly planar without taking into consideration the  $sp^3$ -hybridized methyl group. The layers are separated by around 3.5 Å and there exists no significant interactions between them. However, within layers there exist lines of molecules that run parallel to the *a* axis and in which the molecules of **5** are linked together by hydrogen bonds [N5 $\cdots$ N4<sup>i</sup> 3.045(4) Å and N5 $\cdots$ N1<sup>ii</sup> 3.090(4) Å; symmetry codes, i: 0.5 + *x*, *y*, 0.5 – *z*; ii: –0.5 + *x*, *y*, 0.5 – *z*] that form ring patterns of the form **R2,2(8)** and (of less note) chain graph-sets of the type **C1,1(4)** and **C2,2(6)** (Figure 4).

Generally, and in contrast to the salts of **4** and 1,4DMIT, which form either strong three-dimensional hydrogen-bonding networks or hydrogen-bonded dimers of cations and anions, the salts of **5** and 1,3DMIT form either planar or

Table 2. Selected bond lengths [Å] and angles [°] for the methylated 5-aminotetrazole derivatives.

	<b>5</b>	<b>7</b>	<b>8</b>	<b>9</b>	<b>10</b>	<b>11</b>	<b>12</b>
C2–N2	1.463(4)	1.454(2)	1.464(3)	1.456(2)	1.461(2)	1.457(2)	1.458(2)
C5–N1	1.333(3)	1.325(2)	1.343(2)	1.356(2)	1.357(2)	1.358(2)	1.354(1)
C5–N4	1.341(3)	1.344(2)	1.353(3)	1.331(2)	1.339(2)	1.337(2)	1.333(2)
C5–N5	1.354(3)	1.312(2)	1.322(3)	1.325(2)	1.322(2)	1.325(2)	1.327(2)
N1–N2	1.334(3)	1.334(2)	1.339(2)	1.339(2)	1.335(2)	1.332(2)	1.334(1)
N2–N3	1.304(3)	1.277(2)	1.290(2)	1.287(2)	1.290(2)	1.289(2)	1.286(1)
N3–N4	1.331(3)	1.323(2)	1.330(2)	1.343(2)	1.334(2)	1.340(2)	1.342(1)
C1–N1				1.451(2)	1.456(2)	1.460(2)	1.456(2)
N3–N2–N1	114.9(2)	115.9(1)	116.4(2)	103.1(1)	102.9(1)	103.0(1)	102.9(1)
N2–N3–N4	105.6(2)	102.7(1)	103.0(2)	116.2(1)	116.5(1)	116.3(1)	116.4(1)
N3–N4–C5	106.0(2)	110.6(1)	110.0(2)	102.2(1)	102.3(1)	102.3(1)	101.9(1)
N4–C5–N5	123.6(2)	125.7(1)	124.8(2)	126.3(2)	126.1(1)	126.4(2)	126.7(1)
N1–C5–N4	112.8(2)	107.7(1)	108.4(2)	108.9(1)	108.3(1)	108.4(1)	109.0(1)
N1–C5–N5	123.6(2)	126.4(1)	126.7(2)	124.7(2)	125.4(1)	125.1(2)	124.2(1)
C5–N1–N2	100.6(2)	102.6(1)	102.0(2)	109.4(1)	109.8(1)	109.9(1)	109.5(1)
N1–N2–C2	123.1(3)	122.2(1)	122.1(2)	122.4(2)	121.1(1)	121.0(1)	121.6(1)
N3–N2–C2	122.0(3)	121.8(1)	121.4(2)	121.3(1)	122.2(2)	122.5(1)	121.8(1)
N2–N1–C1				121.5(1)	121.2(1)	120.2(1)	121.9(1)
C5–N1–C1				129.0(1)	128.9(1)	129.7(2)	128.5(1)

Table 3. Medium-to-strong hydrogen bonds for compound **5** and the salts of **5** and 1,3DMIT.<sup>[a]</sup>

D–H...A	D–H [Å]	H...A [Å]	D...A [Å]	D–H...A [°]
<b>5</b>				
N5–H5A...N4 <sup>i</sup>	0.88(3)	2.18(3)	3.045(4)	167(2)
N5–H5B...N1 <sup>ii</sup>	0.79(2)	2.31(3)	3.090(4)	166(2)
<b>7</b>				
N4–H4...N1 <sup>i</sup>	0.76(3)	2.43(3)	3.076(2)	144(2)
N4–H4...O4 <sup>iii</sup>	0.76(3)	2.46(3)	3.013(2)	131(2)
N5–H5A...O3 <sup>iii</sup>	0.79(2)	2.27(2)	3.056(2)	179(2)
N5–H5A...O1 <sup>iii</sup>	0.79(2)	2.56(2)	3.053(2)	121(2)
N5–H5B...O3 <sup>iv</sup>	0.76(2)	2.17(2)	2.918(2)	166(2)
<b>8</b>				
N5–H5A...O1	0.82(3)	2.24(3)	2.983(3)	151(2)
N5–H5B...O1 <sup>i</sup>	0.92(3)	2.11(3)	3.025(3)	176(2)
N5–H5B...O3 <sup>i</sup>	0.92(3)	2.48(3)	3.048(2)	120(2)
N4–H4...O3 <sup>ii</sup>	0.92(3)	1.76(3)	2.670(2)	174(3)
N4–H4...O2 <sup>ii</sup>	0.92(3)	2.60(3)	3.258(3)	130(2)
<b>9</b>				
N5–H5A...O1 <sup>i</sup>	0.82(2)	2.25(2)	3.051(2)	167(2)
N5–H5A...O2 <sup>i</sup>	0.82(2)	2.64(2)	3.052(2)	112(2)
N5–H5B...O2 <sup>ii</sup>	0.83(2)	2.12(2)	2.946(2)	176(2)
<b>10</b>				
N5–H5A...O3 <sup>i</sup>	0.86(2)	2.06(1)	2.925(1)	175(1)
N5–H5B...O1 <sup>ii</sup>	0.81(2)	2.08(2)	2.862(1)	161(1)
<b>11</b>				
N5–H5B...N6 <sup>i</sup>	0.83(3)	2.10(3)	2.919(3)	172(3)
N5–H5A...N8 <sup>ii</sup>	0.88(3)	2.04(3)	2.921(3)	176(3)
<b>12</b>				
N5–H5B...O1 <sup>i</sup>	0.83(3)	2.14(3)	2.952(3)	166(2)
N5–H5B...O3 <sup>i</sup>	0.83(3)	2.34(2)	2.930(3)	126(2)
N5–H5A...O4 <sup>ii</sup>	0.88(2)	2.06(2)	2.908(2)	162(2)

[a] Symmetry codes, for **5**: i:  $0.5 + x, y, 0.5 - z$ ; ii:  $-0.5 + x, y, 0.5 - z$ ; **7**: i:  $-1 + x, y, z$ ; ii:  $-x, -0.5 + y, 0.5 - z$ ; iii:  $1 - x, -y, -z$ ; iv)  $-x, -y, -z$ ; **8**: i:  $0.5 - x, -0.5 + y, 1.5 - z$ ; ii:  $x, -1 + y, z$ ; **9**: i:  $-1 + x, y, z$ ; ii:  $-x, -y, 1 - z$ ; **10**: i:  $x, 0.5 - y, -0.5 + z$ ; ii:  $-x, -y, -z$ ; **11**: i:  $-0.5 + x, 0.5 - y, -0.5 + z$ ; ii:  $1 - x, -y, -z$ ; **12**: i:  $1 - x, 1 - y, 1 - z$ ; ii:  $x, 0.5 - y, 0.5 + z$ .

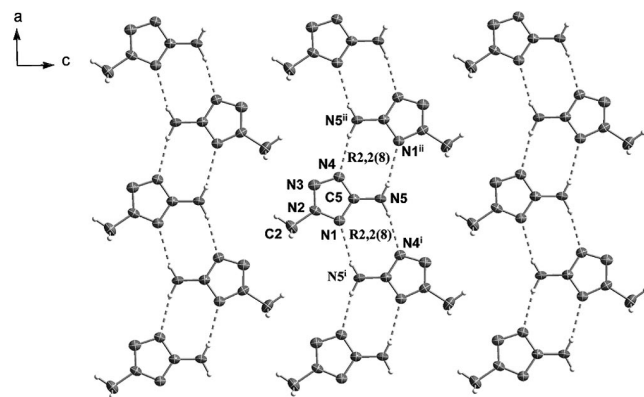


Figure 4. Hydrogen-bonding in a layer in the crystal structure of compound **5**. Symmetry codes, i:  $0.5 + x, y, 0.5 - z$ ; ii:  $-0.5 + x, y, 0.5 - z$ .

wave-shaped layers within which cations and anions are joined by hydrogen-bonding interactions. Also, although the densities of the salts of **5** and 1,3DMIT seem to be, somewhat unexpectedly, slightly higher than those of the analogous salts of **4** and 1,4DMIT, the hydrogen-bonding found in the salts of **5** and 1,3DMIT seem to be generally weaker than that in the salts of **4** and 1,4DMIT. Further

inspection of several of the structures in this study (and in previous work) points to a secondary set of closed-shell interactions between the cations and anions which may be responsible for the higher than expected densities found for the salts of **5** and 1,3DMIT. Lastly, the cation methyl groups in several salts of 1,3DMIT appear, from electron density maps, to be disordered, a circumstance that was not observed for the salts of 1,4DMIT. In addition to disorder in the methyl groups, the dinitramide anion in **12** also appears to suffer from both static and dynamic disorder. Further discussion of the disorder found in this work and its treatment follows below. All of these factors seem to indicate a change in the dominant type of interionic interactions from directional hydrogen-bonding (in the salts of **4** and 1,4DMIT) to less directional electrostatic interactions (in the salts of **5** and 1,3DMIT).

Also, generally speaking, the cations in this study (5-amino-2-methyltetrazolium and 1,3-dimethyl-5-amino-tetrazolium) are all nearly geometrically identical within the limits of structure determination precision (see Table 2) and are also in perfect agreement with the structures determined by Bryden<sup>[26]</sup> and ourselves.<sup>[12]</sup> The geometries of the protonated (in **7** and **8**) and methylated (in **6–12**) cations also show an extremely strong geometric similarity to the neutral parent compound **5**. A slight shortening of the C5–N5 and N2–N3 bonds are observed and a slight lengthening of the C5–N4 (for the salts of **5**) and C5–N1 (for the salts of 1,3DMIT) bonds is also apparent. Differences in bond lengths found in **5** and those found in the salts of **5** and 1,3DMIT are as might be expected for the increased electronic demand of an extra proton or methyl group. The cation structures observed are also, aside from methyl group substitution patterns and the resulting lower symmetry, surprisingly similar to those of the salts of **4** and 1,4DMIT.

As stated above, the strength and extent of the hydrogen-bonding networks observed in the salts of **5** and 1,3DMIT seem to be less than those found in the salts of **4** and 1,4DMIT. Specifically, compounds **7** and **8** both form only five hydrogen bonds each (see Table 3 and Figures 5 and 6) as opposed to the seven hydrogen bonds formed in analogous salts of **4**. Because **8** crystallizes in a layer structure, hydrogen-bonding in **8** only occurs between cations and anions lying in the same plane. In addition, cations and anions form hydrogen-bonded bands within each plane, between which only non-polar interactions between the methyl groups are observed. Non-dimeric hydrogen-bonding patterns are observed only at the secondary level and are mainly of the chain variety with the designators **C1,2(X)** ( $X = 4, 6$ ) and **C2,2(X)** ( $X = 6–8$ ). Each nitrate anion also chelates two protons (see Figure 5 for details) forming **R2,1(4)** ring systems. The five hydrogen bonds in **7** form a three-dimensional network composed mainly of common hydrogen-bonding patterns such as **C1,1(4)**, **C1,2(4)**, **C2,2(8)**, **D3,2(7)** and **D3,3(11)**. Of note are the chain patterns observed at the primary level formed by the N4...N1<sup>i</sup> hydrogen bond (symmetry code, i:  $-1 + x, y, z$ ), which connects only the cations in the structure along the *a* axis and

the **R2,1(4)** ring patterns, which are comparable to those formed in the nitrate salt **8**. The two latter networks are represented in Figure 6.

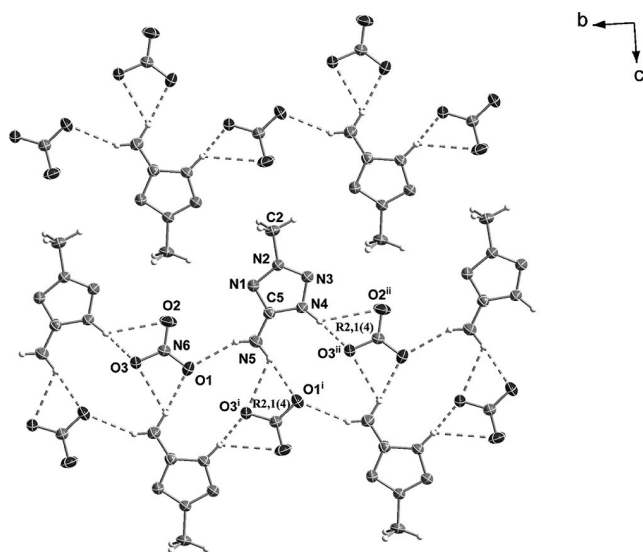


Figure 5. Hydrogen-bonding in a layer of nitrate salt **8**. Symmetry codes, i:  $0.5 - x, -0.5 + y, 1.5 - z$ ; ii:  $x, -1 + y, z$ .

The salts of **5** show a very similar number of hydrogen bonds to the analogous salts of 1,4DMIT (see Table 3 and Figure 8, Figure 9, Figure 10 and Figure 11). The hydrogen-bonding patterns formed in the salts of 1,3DMIT are generally quite simple due to the small number of interactions observed. For **6**, **9** and **10**, similar hydrogen-bonded chains of cations and anions **C1,2(4)**,<sup>[12]</sup> **C2,2(6)** (Figure 8) and **C2,2(6)** (Figure 9), respectively, are observed. The relationship between the structures of **6** and **10** seems, on account of space group and unit cell similarities, to extend beyond hydrogen-bonding patterns to overall packing. Both **6** and **10** crystallize in the orthorhombic space group *Pbca* forming very similar zig-zag arrangements of hydrogen-bonded chains of cations and anions, as shown in Figure 7.

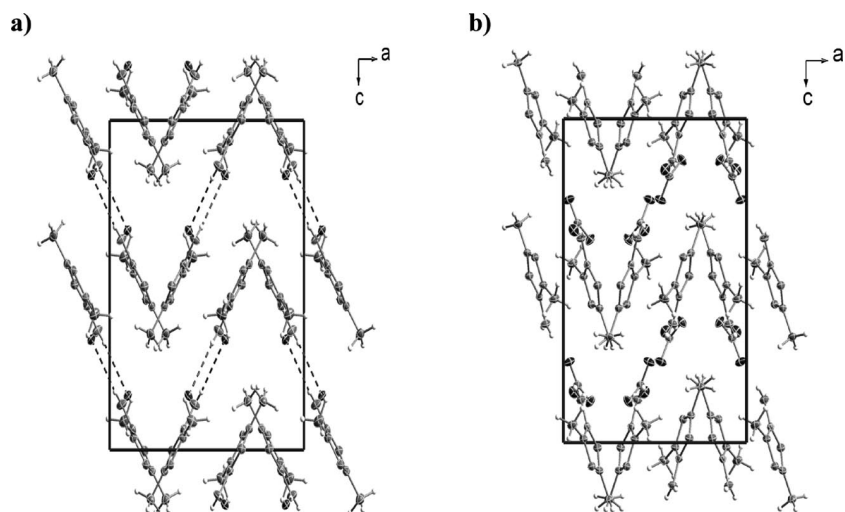


Figure 7. View of the unit cells of a) the iodide salt **6** and b) the nitrate salt **10** along the *b* axis showing the formation of zig-zag chains. The hydrogen bonds in the unit cell of **10** have been omitted for simplicity.

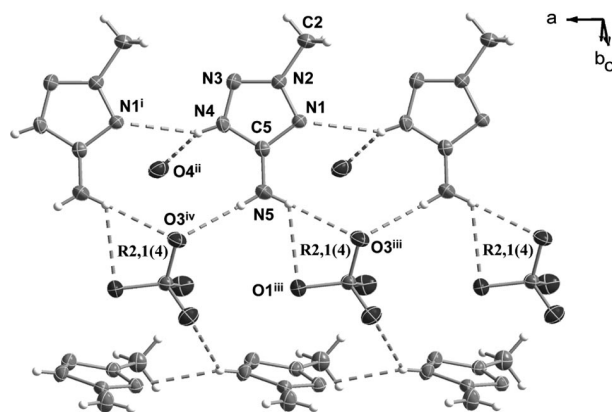


Figure 6. Section of the hydrogen-bonding in the crystal structure of perchlorate salt **7**. Some of the perchlorate anion atoms have been omitted for simplicity. Symmetry codes, i:  $-1 + x, y, z$ ; ii:  $-x, -0.5 + y, 0.5 - z$ ; iii:  $1 - x, -y, -z$ ; iv:  $-x, -y, -z$ .

In both structures the crystallographic *b* axis is quite similar (see Table S1), which seems to be a result of the fact that the hydrogen-bonded chains of cations and anions run in the *b* direction. As can be seen in Figure 7, the angle between neighbouring chains is slightly higher in **6** (ca.  $70^\circ$ ) than in **10** (ca.  $50^\circ$ ). This difference can be explained by the spherical iodide anions in contrast to the planar nitrate anions. This structural difference has the greatest effect on the crystallographic *a* axis and a lesser effect on the *c* axis, as shown by the lattice parameters listed in Table S1. Figure 8 (a) shows the hydrogen-bonding between the cation and the nitrate anion (Table 3). The hydrogen bonds formed by the two hydrogen atoms on N5 and one of the oxygen atoms of the nitrate anions are similar in length [ $N5 \cdots O3^i$  2.925(1) Å and  $N5 \cdots O1^{ii}$  2.862(1) Å; symmetry codes, i:  $x, 0.5 - y, -0.5 + z$ ; ii:  $-x, -y, -z$ ] and show two **D1,1(2)** dimeric interactions and the **C2,2(6)** chain motif mentioned above, which includes the amino group ( $NH_2$ ) of the cation and an  $NO_2$  moiety of the anion. From the lateral view (Figure 8, b) the formation of wave-like layers along the *b* axis can be seen.

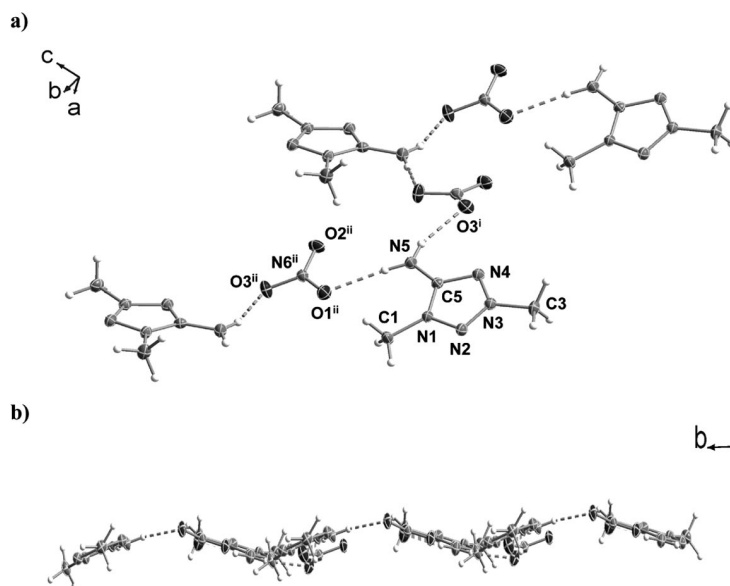


Figure 8. a) **C2,2(6)** chain networks in the crystal structure of nitrate salt **10** and b) lateral view of one of the waved-layers formed along the *b* axis. Symmetry codes, i:  $x, 0.5 - y, -0.5 + z$ ; ii:  $-x, -y, -z$ .

The planar cation and the tetrahedral perchlorate anion in compound **9** interact, forming cation–anion dimers joined by an **R4,4(12)** pattern identical to those formed in the analogous salt of 1,4DMIT (Figure 9). This (large) ring graph-set is formed by the superposition of two smaller ring patterns with the labels **R2,1(4)** and **R4,4(8)**. In analogy with the other two salts of 1,3DMIT described above, infinite zig-zag chains are formed, this time along the *c* axis. Lastly, there exists no hydrogen-bonding between chains, but only weak covalent interactions.

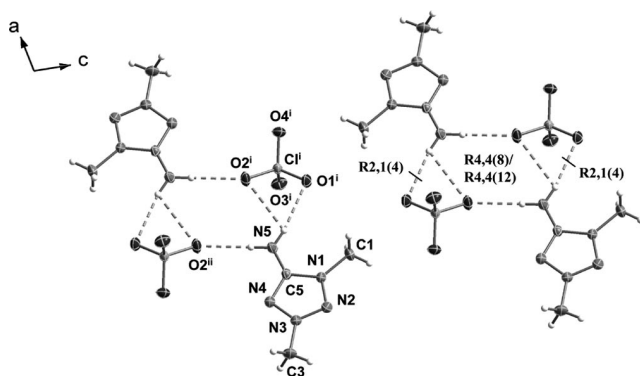


Figure 9. Formation of ring graph-sets in the crystal structure of perchlorate salt **9**. Symmetry codes, i:  $-1 + x, y, z$ ; ii:  $-x, -y, 1 - z$ .

Compound **11** is formed by the planar 5-amino-1,3-dimethyltetrazolium cation and a linear azide anion [N6–N7–N8 179.7(2)°]. However, with different unit cell parameters and symmetry, it does not show the strong similarities observed between **6** and **10** discussed above. A view along the *b* axis of the compound shows wave-like chains of alternating cations and anions that form (Figure 10, a). Among these layers there are no hydrogen bonds. The hydrogen-

bonding in such a layer is depicted in Figure 10b. There exist two **D1,1(2)** dimeric interactions and a **C2,2(6)** chain motif, which extends from one of the protons on N5 to N8<sup>ii</sup>. The length of the hydrogen bond between the atoms N5 and N6<sup>i</sup> [N5⋯N6<sup>i</sup> 2.919(3) Å; symmetry code, i:  $-0.5 + x, 0.5 - y, -0.5 + z$ ] is very similar to that between the atoms N5 and N8<sup>ii</sup> [N5⋯N8<sup>ii</sup> 2.921(3) Å; symmetry code, ii:  $1 - x, -y, -z$ ].

The anions in this study (iodide, nitrate, perchlorate, azide and dinitramide) are structurally well characterized and, aside from the dinitramide anion in **12**, show no unusual structural features. From the X-ray structure of **12**, the dinitramide appears to suffer both considerable static and dynamic disorder, conditions not previously observed in structures involving the dinitramide anion.<sup>[8,19,28]</sup> The presence of disorder is not particularly surprising given that the interactions between the delocalized cation and anion in **12** is not particularly strong (as indicated by the very low melting point of **12**). Therefore, static disorder results from the lack of a single energetically preferred arrangement of cations and anions and dynamic disorder from the lack of strong directional interactions between O2 and O3 of the dinitramide anion and the cation. Although a complete analysis of the hydrogen-bonding pattern found in **12** is difficult on account of the disordered anion, it is apparent that **12** forms the same helical hydrogen-bonded chains of cations and anions as was observed in the dinitramide salt of 1,4DMIT (Figure 11).<sup>[8]</sup> The planar cation and the pyramidal dinitramide anion interact to form three strong hydrogen bonds of different lengths [N5⋯O1<sup>i</sup> 2.952(3) Å, N5⋯O3<sup>i</sup> 2.930(3) Å and N5⋯O4<sup>ii</sup> 2.908(2) Å; symmetry codes, i:  $1 - x, 1 - y, 1 - z$ ; ii:  $x, 0.5 - y, 0.5 + z$ ]. The N5H<sub>2</sub> group forms two hydrogen bonds with the oxygen atoms labelled as O1<sup>i</sup> and O3<sup>i</sup>, which results in an **R2,1(6)** ring graph-set. Furthermore, three **D1,1(2)** dimeric interactions,

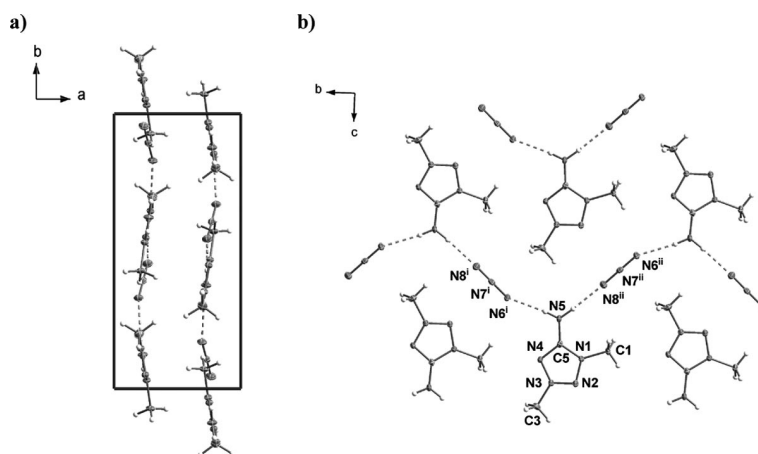


Figure 10. a) Waves of anions and cations in the unit cell of azide salt **11** along the *b* axis and b) view of the hydrogen-bonding within a layer (dotted lines). Symmetry codes, i:  $-0.5 + x, 0.5 - y, -0.5 + z$ ; ii:  $1 - x, -y, -z$ .

one **C2,2(6)** and one **C2,2(8)** chain patterns occur. The cations and anions form layers, which alternate and there exist hydrogen bonds between and within these layers.

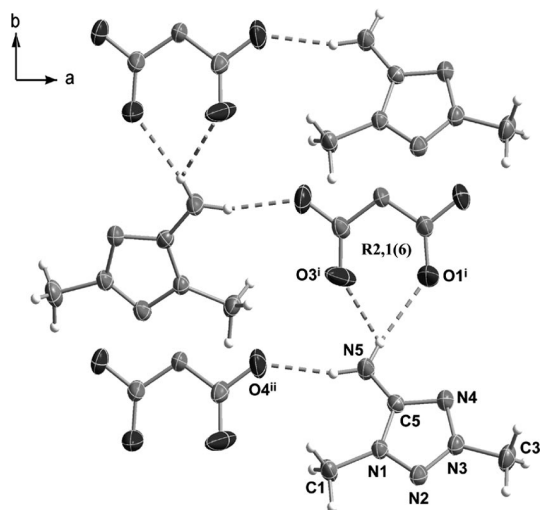


Figure 11. Hydrogen-bonding in the crystal structure of dinitramide salt **12**. Symmetry codes, i:  $1 - x, 1 - y, 1 - z$ ; ii:  $x, 0.5 - y, 0.5 + z$ .

The above observations concerning hydrogen-bonding seem to suggest weaker interionic interactions in the salts of **5** and 1,3DMIT compared with those observed in the salts of **2** and 1,4DMIT. However, as noted above, the densities of the salts of **5** and 1,3DMIT are generally similar to or higher than those of the salts of **4** and 1,4DMIT, which suggests some other form of cation–anion interaction. Further inspection of the structures indicates the presence of additional cation–anion interactions in compounds **7**, **9**, **10** and **12**. These interactions appear to be similar in nature to the closed-shell interactions<sup>[29]</sup> between anion and cation that we previously identified in 1,5-diamino-4-methyltetrazolium dinitramide.<sup>[28]</sup> Such interactions might have strengths similar to those of hydrogen bonds, which would explain the discrepancies between the observed cation–anion interaction strengths and the densities. The distances

(within or close to the sum of the van der Waals radii) between the cations and anions found in **7**, **9**, **10** and **12** are tabulated in Table S2.

### Energetic Properties

The thermal stability (melting and decomposition points from DSC measurements) and the sensitivity to friction, impact, electrostatic discharge and thermal shock of each energetic salt studied were determined experimentally (Tables 4 and 5). The impact sensitivity tests were carried out according to STANAG 4489<sup>[30]</sup> modified with the instructions<sup>[31]</sup> for using a BAM (Bundesanstalt für Materialforschung)<sup>[32]</sup> drop hammer. The friction sensitivity tests were carried out according to STANAG 4487.<sup>[33]</sup> Additionally, the constant volume energy of combustion of each material was determined experimentally by oxygen bomb calorimetry and also predicted on the basis of calculated electronic energies (see the Computational Methods section and Table S3 in the Supporting Information) and an estimation of the lattice enthalpy<sup>[34,35]</sup> (Table S4), as described previously.<sup>[36]</sup>

DSC measurements on samples of around 1 mg of each energetic compound in this study (**7**, **8** and **10–12**) show a wide range of melting points, from 58 (**12**) to 171 °C (**11**), and decomposition points, between 161 (**8**) and 285 °C (**9**) (Table 4). As might be expected for a lower symmetry cation, the salts of **5** and 1,3DMIT generally have slightly lower melting points than the analogous salts of **4** and 1,4DMIT.<sup>[8]</sup> In a comparison with commonly used explosives like TNT and RDX (1,3,5-trinitroperhydro-1,3,5-triazine), **12** melts at a temperature lower than TNT (81 °C) and belongs to the class of compounds known as ionic liquids (m.p. <100 °C), whereas the remaining compounds have melting points higher than TNT but lower than RDX (204 °C).<sup>[38]</sup> Compounds **7**, **8**, **10** and **12** decompose at lower temperatures than RDX (230 °C), whereas salts **9** and **11** decompose at a higher temperature than RDX and slightly below the decomposition point of TNT (300 °C). In

Table 4. Physicochemical properties of the energetic salts.

	7	8	9	10	11	12
Formula	C <sub>2</sub> H <sub>6</sub> ClN <sub>5</sub> O <sub>4</sub>	C <sub>2</sub> H <sub>6</sub> N <sub>6</sub> O <sub>3</sub>	C <sub>3</sub> H <sub>8</sub> ClN <sub>5</sub> O <sub>4</sub>	C <sub>3</sub> H <sub>8</sub> N <sub>6</sub> O <sub>3</sub>	C <sub>3</sub> H <sub>8</sub> N <sub>8</sub>	C <sub>3</sub> H <sub>8</sub> N <sub>8</sub> O <sub>4</sub>
Mol. mass [g mol <sup>-1</sup> ]	199.57	162.11	213.59	176.15	156.17	220.17
T <sub>m</sub> [°C] <sup>[a]</sup>	125	123	132	150	171	58
T <sub>d</sub> [°C] <sup>[b]</sup>	196	161	285	199	282	168
N [%] <sup>[c]</sup>	35.1	51.8	32.8	47.7	71.8	50.9
N + O [%] <sup>[d]</sup>	67.1	81.4	62.8	74.9	71.8	80.0
Ω [%] <sup>[e]</sup>	-20.0	-39.5	-41.2	-63.6	-102.5	-43.6
ρ [g cm <sup>-3</sup> ] <sup>[f]</sup>	1.844	1.620	1.631	1.569	1.479	1.575
ΔU <sub>comb.</sub> [cal g <sup>-1</sup> ] <sup>[g,h]</sup>	-2250(40) [-2346]	-2620(20) [-2587]	-2735(40) [-2937]	-3250(35) [-3271]	-4430(35) [-4377]	-2750(35) [-2848]
ΔU <sub>f</sub> <sup>o</sup> [kJ kg <sup>-1</sup> ] <sup>[h,i]</sup>	3765(160) [2752]	950(90) [794]	2610(170) [2518]	520(150) [612]	3670(155) [3560]	1060(150) [1474]
ΔH <sub>f</sub> <sup>o</sup> [kJ kg <sup>-1</sup> ] <sup>[h,i]</sup>	3670(160) [2666]	810(90) [680]	2505(170) [2425]	380(150) [493]	3480(155) [3433]	930(150) [1362]

[a] Chemical melting point. [b] Decomposition point (DSC onsets) from measurement with  $\beta = 5 \text{ }^\circ\text{C min}^{-1}$ . [c] Nitrogen content. [d] Combined nitrogen and oxygen contents. [e] Oxygen balance according to ref.<sup>[37]</sup>. [f] Density from X-ray measurements. [g] Constant volume energy of combustion determined experimentally (oxygen bomb calorimetry). [h] Uncertainty in parentheses and calculated values (from electronic energies) in brackets. [i] Standard energy of formation determined experimentally (back-calculated from  $\Delta U_{\text{comb.}}$ ). [j] Standard enthalpy of formation determined experimentally.

Table 5. Initial safety testing results, predicted energetic performance of the energetic salts using the EXPLO5 computer code<sup>[41]</sup> and comparison with commonly used energetic materials.

	T <sub>ex</sub> [K] <sup>[a]</sup>	V <sub>0</sub> [L kg <sup>-1</sup> ] <sup>[b]</sup>	P <sub>det</sub> [GPa] <sup>[c]</sup>	D [m s <sup>-1</sup> ] <sup>[d]</sup>	Impact [J] <sup>[e]</sup>	Friction [N] <sup>[e]</sup>	ESD (+/-) <sup>[f]</sup>	Thermal shock
7					1	6	+	explodes
8	3771 [3698]	838 [837]	25.9 [25.5]	8150 [8109]	>30	>360	-	burns
9					3.5	24	+	deflagrates
10	3234 [3277]	826 [826]	22.6 [22.7]	7850 [7864]	>30	>360	-	burns
11	2880 [2837]	835 [834]	23.5 [23.2]	8436 [8393]	>30	>360	-	deflagrates
12	3769 [3997]	825 [826]	23.7 [25.3]	7869 [8097]	15	>360	-	deflagrates
TNT	3736	620	20.5	7171	15	355	0.57 J <sup>[g]</sup>	burns
RDX	4334	795	34.0	8885	7.4	120	0.15 J <sup>[g]</sup>	burns

[a] Temperature of the explosion gases. [b] Volume of the explosion gases. [c] Detonation pressure. [d] Detonation velocity. [a]–[d] Experimental values (from bomb calorimetry) and calculated values (from electronic energies) are given in brackets. [e] Tests carried out according to BAM methods (see refs.<sup>[40,42,43]</sup>). [f] Rough sensitivity towards electrostatic discharge: + sensitive, – insensitive. [g] From ref.<sup>[44]</sup>.

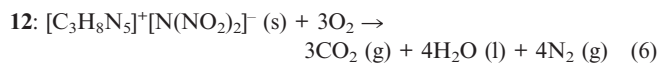
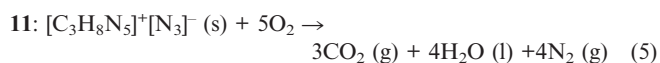
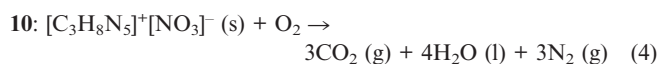
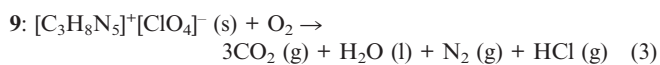
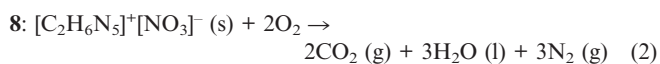
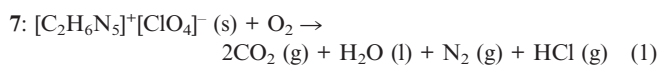
In addition to DSC analysis, all compounds were tested by placing a small sample (ca. 0.5–1.0 mg) of compound in a flame (Figure S4). In the case of the very sensitive perchlorate salt **7**, the sample exploded. For **9–12** deflagration (rapid combustion accompanied by a hissing sound) without explosion was observed whereas the nitrate derivatives **8** and **10** simply burn normally. From these “flame test” observations it can be deduced that the compounds in this study, composed of a higher percentage of nitrogen or containing a highly oxidant anion (e.g., perchlorate or dinitramide), are more sensitive to thermal shock than might have been expected.

Compounds **7**, **8** and **10–12** are highly endothermic compounds, as expected due to the large number of energetic N–N and C–N bonds,<sup>[39]</sup> that show relatively low sensitivities. Data collected for friction, impact and electrostatic discharge sensitivity testing are summarized in Table 5. The compounds in this study are slightly less or as equally sensitive to physical and electrical stimuli as the analogous salts of **4** and 1,4DMIT. Within the series of salts based on **5** and 1,3DMIT a trend for increasing sensitivity with decreasingly negative oxygen balance is observed, as was the case for the “flame test.” Also, each compound was roughly tested for sensitivity towards electrostatic discharge

by spraying sparks across a small (3–5 crystals) sample of material using a tesla coil (ESD testing). Apart from the sensitive perchlorate salts **7** and **9**, all compounds failed to explode under these conditions. Once again, a comparison with the properties of TNT and RDX is useful to assess the energetic salts in this study. The perchlorate-free compounds (**8**, **10**, **11** and **12**) are less sensitive to both friction and impact than TNT (15 J) and RDX (7.4 J),<sup>[38]</sup> whereas the perchlorate salts **7** and **9** are quite sensitive to both friction and impact with sensitivities similar to those of primary explosives and very sensitive secondary explosives. All of the compounds are most likely less sensitive to electrostatic discharge than both TNT and RDX, although this was not unambiguously confirmed by quantitative testing. Lastly, all of the compounds in this study, except for the perchlorate salts **7** and **9**, are safe for transport under the UN Recommendations on the Transport of Dangerous Goods, as described in ref.<sup>[40]</sup>

Because the performance of the new energetic materials is also of considerable interest, the EXPLO5 computer code was used to calculate the detonation velocity and pressure of the CHNO explosives in this work on the basis of the molecular formula, density (from X-ray analysis) and energy of formation ( $\Delta U_f^o$ , both experimental and calculated)

of each material. Therefore, the energies of formation of **7**, **8** and **10–12** were back-calculated from the constant volume energies of combustion by first converting them into standard enthalpies of combustion and then, on the basis of the combustion equations [see Equations (1)–(6)] and Hess's Law and by incorporating the known standard heats of formation for water and carbon dioxide<sup>[45]</sup> and a correction for change, into gas volume during combustion.<sup>[46]</sup> No correction was applied for the non-ideal formation of nitric acid (generally ca. 5% of the nitrogen atoms react to form nitric acid). Owing to the reasonably large uncertainty inherent in the experimental combustion measurements of energetic materials, the thermochemical data ( $\Delta U_{\text{comb}}$ ,  $\Delta U_{\text{f}}^{\circ}$  and  $\Delta H_{\text{f}}^{\circ}$ ) for each compound were predicted on the basis of known methods, utilizing calculated electronic energies and an approximation of lattice enthalpy<sup>[34,35]</sup> to validate the experimentally determined values. The results of the thermochemical measurements and calculations are presented in Tables 4 and 5 in brackets.



The experimentally determined thermochemical data were then used in conjunction with the EXPLO5 computer code to predict the detonation parameters of each CHNO compound in this study. The program uses the Becker–Kistiakowsky–Wilson equation of state (BKWN-EOS) for gaseous detonation products and the Cowan–Fickett equation of state for solid carbon.<sup>[41,47]</sup> The following values for the empirical constants in the BKWN-EOS equation,  $\alpha = 0.5$ ,  $\beta = 0.176$ ,  $\kappa = 14.71$  and  $\theta = 6620$ , were used for all compounds in this study. The results of the calculations are shown in Table 5, along with the results of EXPLO5 calculations for TNT and RDX. From these predictions made by using the BKWN-EOS parameters given above and the known data for TNT and RDX, it would seem that the detonation velocity and most likely the pressure as well are slightly overestimated. Taking into account this systematic overestimation, the performance of all of the compounds assessed in this study is expected to fall between that of TNT (7171 ms<sup>-1</sup>, 20.5 GPa) and RDX (8885 ms<sup>-1</sup>, 34.0 GPa). The performance of the salts of **5** and 1,3DMIT seem, surprisingly, to exceed that of the salts of **4** and 1,4DMIT. It seems that in spite of the lower symmetry of the cation of 1,3DMIT, generally slightly higher densities

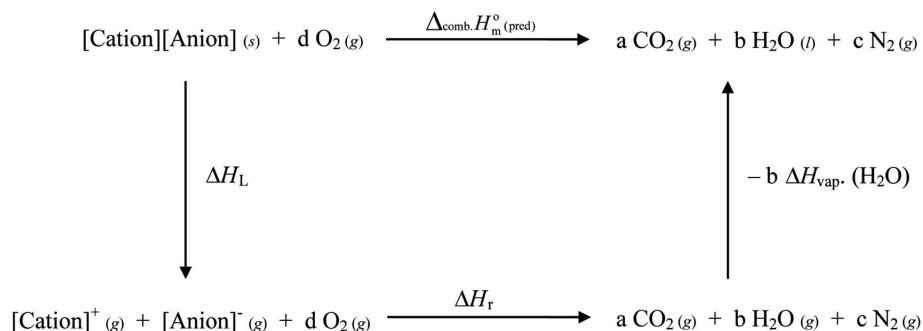
are observed for the salts of 1,3DMIT compared with the salts of 1,4DMIT, leading to higher predicted performances for the salts of 1,3DMIT due to the strong dependence of this property on density.<sup>[48]</sup> The experimentally determined detonation parameters are in excellent agreement with those predicted on the basis of electronic energies (see the Computational Methods section). The nitrogen-rich azide salt **11** has the highest performance of all the materials in this study (8436 ms<sup>-1</sup>, 23.5 GPa) regardless of its relatively low density (1.479 g cm<sup>-3</sup>) and yet it is insensitive to impact and friction. The nitrate salt **8** is relatively well oxygen balanced ( $\Omega = -39.5\%$ ), comparable to RDX ( $\Omega = -21.6\%$ ), and shows a reasonably high performance (8150 ms<sup>-1</sup>, 25.9 GPa), greater than that of nitrogen-rich salts with the 5,5'-azotetrazolate anion ( $[\text{C}_2\text{N}_{10}]^{2-}$ ).<sup>[7a,49]</sup>

It is known that the performance of a material reaches its maximum value when the oxygen balance is approximately neutral. Owing to the generally highly negative oxygen balance of the CHNO compounds **8**, **10**, **11** and **12**, we calculated detonation parameters for mixtures of these compounds with an oxidizer, namely, ammonium nitrate (AN) and ammonium dinitramide (ADN), to further increase the performance relative to the stand-alone energetic materials. The results of the calculations are summarized in Tables S5 and S6. AN slightly increases the detonation parameters of the compounds (ca. 8200–8300 ms<sup>-1</sup> and ca. 26 GPa), whereas ADN is predicted to increase the performance much more significantly (ca. 8700–8900 ms<sup>-1</sup> and ca. 31–32 GPa).

## Computational Methods

All quantum chemical calculations were carried out with the Gaussian 03W software package.<sup>[50]</sup> The electronic energies for all of the anions and the 2-methyl-5-aminotetrazolium and 5-amino-1,3-dimethyltetrazolium cations were calculated by using Møller–Plesset perturbation theory truncated at the second order (MP2)<sup>[51]</sup> and were used unscaled. The results of the MP2 electronic energy calculations are tabulated in Tables S3 and S4 of the Supporting Information. For all atoms in all calculations, the correlation-consistent polarized valence double-zeta basis set (cc-pVDZ) was used.<sup>[52,53]</sup>

Based on the Born–Haber cycle shown in Scheme 3,<sup>[54]</sup> the heat of formation of an ionic compound can be simplified by subtracting the lattice energy of the salt ( $\Delta H_{\text{L}}$ ) from the sum of the heats of formation of the cation and anion (at standard conditions) according to Equation (7).  $\Delta H_{\text{L}}$  (kJ mol<sup>-1</sup>) can be predicted by using Jenkins' equation [Equation (8)],<sup>[34]</sup> where  $n_x$  and  $n_y$  depend on the nature of cation and anion, respectively, and have a value of 6 for non-linear polyatomic ions. The potential energy ( $U_{\text{POT}}$  in kJ mol<sup>-1</sup>) can be readily calculated from the density of the material ( $\rho$  in g cm<sup>-3</sup>), the mass of the chemical formula ( $M$  in g) and the coefficients  $\gamma$  (kJ mol<sup>-1</sup> cm<sup>-1</sup>) and  $\delta$  (kJ mol<sup>-1</sup>), which take their values from the literature,<sup>[34]</sup> according to Equation (9).



Scheme 3. Born–Haber energy cycle for calculating the heat of formation of an ionic CHNO compound.

Table 6. Predicted decomposition gases and heats of explosion of methylated 5-aminotetrazole derivatives and comparison with known high explosives (using the ICT code).<sup>[a]</sup>

	CO <sub>2</sub>	H <sub>2</sub> O	N <sub>2</sub>	CO	H <sub>2</sub>	NH <sub>3</sub>	CH <sub>4</sub> /HC <sup>[b]</sup>	HCl	C	$\Delta H_{\text{ex}}$ [cal g <sup>-1</sup> ] <sup>[c]</sup>
<b>7</b>	167.7	213.2	345.6	16.0	0.2	6.3	182.7	0.3	67.4	2164
<b>8</b>	54.8	281.2	495.8	11.0	0.7	27.0	1.3	0.6	127.2	1391
<b>9</b>	80.5	260.7	315.0	16.5	0.7	15.3	1.5/170.7	0.4	138.3	1876
<b>10</b>	18.4	286.7	427.7	7.6	1.5	59.6	6.1	0.8	191.3	1253
<b>11</b> <sup>[d]</sup>	(–)	(–)	545.2	(–)	3.7	208.8	42.9	1.2	198.1	1004
<b>12</b>	55.7	273.4	486.7	12.5	0.8	26.6	1.8	0.6	141.4	1395
TNT <sup>[d]</sup>	318.1	184.8	182.2	47.0	0.6	3.2	1.2	(–)	262.0	1350
RDX <sup>[d]</sup>	292.6	232.8	373.9	21.5	0.2	5.1	(–)	0.3	72.7	1593

[a] The amount of gas formed at 298 K is given in grams of gas per kilogram of energetic compound. [b] CH<sub>4</sub> for compounds **8** and **10**–**12** and HCl for compounds **7** and **9**. [c] Heat of explosion. [d] (–) gas not predicted by the code.

$$\Delta H_f^\circ (\text{ionic compound, 298 K}) = \Sigma \Delta H_f^\circ (\text{cation, 298 K}) + \Sigma \Delta H_f^\circ (\text{anion, 298 K}) - \Delta H_L \quad (7)$$

$$\Delta H_L = U_{\text{POT}} + [a(n_x/2 - 2) + b(n_y/2 - 2)]RT \quad (8)$$

$$U_{\text{POT}} = \gamma(\delta/M)^{1/3} + \delta \quad (9)$$

## Decomposition Gases

The ICT thermodynamic code<sup>[55]</sup> can be used to predict the gaseous products formed upon decomposition and/or explosion of an energetic compound as well as its heat of explosion. By using the experimentally determined heats of formation (back-calculated from the heats of combustion), the density (from X-ray analysis) and the molecular formula, the explosion products and the corresponding heats of explosion were calculated for all energetic compounds studied in this work. The results are tabulated in Table 6 together with analogous calculations for commonly used high explosives.

Compounds **7**, **8** and **10**–**12** have (generally) high nitrogen contents varying in the range of around 35–72% and thus the major decomposition product predicted by the code is molecular nitrogen. The amounts of nitrogen gas formed add to up to 545.2 g kg<sup>-1</sup> for the nitrogen-rich azide salt **11** and decrease accordingly with lower nitrogen content for the rest of the compounds. Apart from the CHN compound **11**, which cannot be oxidized to form water, for the remainder of the compounds this is expected to be the second major decomposition product (ca. 210–280 g kg<sup>-1</sup>). As expected, the higher oxygen content of the perchlorate salts **7** and **9** anticipates relatively large

amounts of carbon being oxidized to carbon dioxide. Owing to the negative oxygen content of the compounds studied here (ca. –20 to –100%) not all the carbon atoms can be oxidized and carbon soot is expected to form in amounts larger than for RDX, but lower than for TNT. On the other hand, excepting compound **11**, the rest of the salts have predicted heats of explosion higher than that of TNT and the perchlorate salts **7** and **9** are predicted to show higher values than RDX. This can be explained by the high density and high endothermicity of the compounds due to the perchlorate anion. Unfortunately, relatively large amounts of (toxic) hydrochloric acid are anticipated by the ICT code, which might limit their interest as environmentally friendly replacements for commonly used energetic compounds. The formation of a small cloud of hydrochloric acid was observable in the “flame test” of compound **9** (see Figure S4). In any case, the formation of large amounts of environmentally benign nitrogen gas for the rest of the materials is a clear advantage with respect to classical energetic compounds and together with the properties summarized above might also make the materials prospective candidates for future applications as high-explosive compounds, gas generators or components of propellants or propellant charges.<sup>[56–59]</sup>

## Conclusions

An improved synthesis of 5-amino-2-methyltetrazole (**5**) has been developed in this work. Tetrazole **5** can either be protonated or methylated leading to the synthesis of a fam-

ily of energetic salts based on the new 2-methyl- and 5-amino-1,3-dimethyltetrazolium cations and nitrate, perchlorate, azide and dinitramide anions, which are analogous to our previously reported salts of **4** and 1,4DMIT. The new compounds have been fully characterized, including the determination of their solid-state structures. An insight into the structure of the compounds in solution was gained by  $^{15}\text{N}$  NMR measurements, which also give an insight into the high acidity of the cations of **5** and 1,3DMIT. The crystal structures have been discussed, making use of the graph-set formalism, and show, in general, weak interactions between cations and anions, as already anticipated by analysis of the vibrational spectra. Nevertheless, the compounds show, as a rule, density values that are slightly higher than those of the salts of **4** and 1,4DMIT, regardless of the asymmetric substitution pattern in the cation of 1,3DMIT. This better efficiency in packing can be explained by closed-shell interactions, which are similar in strength to hydrogen bonds and contribute to the unexpectedly larger detonation parameters of the salts of **5** and 1,3DMIT in comparison with the salts of **4** and 1,4DMIT, while having similar sensitivity values. The asymmetric substitution pattern of the cation of 1,3DMIT results in slightly lower decomposition temperatures and a drop in the melting points. Interestingly, the dinitramide salt **12** melts at 58 °C and thus is classified as an ionic liquid with a high performance, whereas the azide salt **11** has a detonation velocity perfectly comparable to commonly used high-performing high explosives such as PETN or RDX in addition to a large liquid range (>100 °C) and it has the advantage that it is neither impact nor friction sensitive. As expected from the high nitrogen content of the compounds, large amounts of nitrogen are predicted by the ICT code, which makes the compounds (excepting the perchlorate salts **7** and **9**) attractive as environmentally friendly replacements for typically used energetic materials. Lastly, the relatively high performance of the remainder of the compounds together with excellent combined oxygen and nitrogen contents and low sensitivities make the materials and, in particular compounds **11** and **12**, very attractive as prospective candidates for future energetic applications.

## Experimental Section

**General:** See the Supporting Information

**Caution:** Although we experienced no difficulties with the compounds described herein, silver azide, dinitramides, aminotetrazoles and their derivatives are energetic materials and tend to explode under certain conditions. Appropriate safety precautions should be taken, especially when these compounds are prepared on a larger scale. Laboratories and personnel should be properly grounded and safety equipment such as Kevlar gloves, leather coats, face shields and ear plugs are highly recommended.

**Synthesis of *N*-(1*H*-Tetrazol-5-yl)phthalimide (**2**):** Phthalic anhydride (5.920 g, 39.99 mmol) was dissolved in glacial acetic acid (20 mL) at an oil bath temperature of 90 °C. Anhydrous 5-amino-1*H*-tetrazole (3.381 g, 40.24 mmol) was added in one portion and the mixture was heated at reflux to form a clear colourless solution,

which was boiled for 2 h. After 1 h reaction time a white precipitate formed, the oil bath was switched off and the precipitated solid was separated by filtration at room temperature, washed with acetone and allowed to dry overnight (7.894 g, 92%).  $\text{C}_9\text{H}_5\text{N}_5\text{O}_2$  (215.04): calcd. C 50.22, H 2.34, N 32.56; found C 50.24, H 2.35, N 32.82. M.p. (uncorrected): 260–262 °C (dec.). MS (EI<sup>+</sup>, 70 keV, >5%):  $m/z = 215.2$  [M + H]<sup>+</sup>.  $^1\text{H}$  NMR ([D<sub>6</sub>]DMSO, 400.18 MHz, TMS):  $\delta = 14.87$  (s, 1 H, NH), AA'BB' spin system: 7.83, 7.77 (m, 4 H, arom-H) ppm.  $^{13}\text{C}\{^1\text{H}\}$  NMR ([D<sub>6</sub>]DMSO, 100.52 MHz, TMS):  $\delta = 164.7$  (2 C, C-2/C-9), 149.5 (1 C, C-1), 135.6 (2 C, C-5/C-6), 131.1 (2 C, C-3/C-8), 124.3 (2 C, C-4/C-7) ppm. Raman:  $\tilde{\nu}$  (rel. int.) = 3090 (15), 3071 (18), 1804 (100), 1758 (5), 1731 (4), 1617 (32), 1606 (26), 1428 (8), 1361 (11), 1295 (5), 1248 (13), 1183 (44), 1072 (10), 1013 (46), 879 (11), 823 (4), 795 (2), 683 (36), 666 (3), 576 (15), 364 (19), 305 (8), 256 (10), 204 (16), 185 (11), 166 (8), 123 (3) cm<sup>-1</sup>.

**Synthesis of *N*-(2-Methyltetrazol-5-yl)phthalimide (**3**):** Tetrazole **2** (1.508 g, 7.01 mmol) was suspended in water (25 mL) and sodium hydrogen carbonate (0.595 g, 7.08 mmol) was added. The suspension was carefully heated until no more gas was evolved and all the material dissolved. A solution of methyl iodide (1.221 g, 8.60 mmol) in acetone (10 mL) was added and the mixture was allowed to react at 70 °C for 4 h. After 1 h reaction time a white crystalline precipitate had formed, extra methyl iodide (1.023 g, 8.67 mmol) was added and the reaction was continued for a further 4 h. The reaction mixture was left to cool to room temperature and the precipitated solid was filtered off, washed with acetone and dried under vacuum (0.976 g, 61%).  $\text{C}_{10}\text{H}_7\text{N}_5\text{O}_2$  (229.06): calcd. C 52.39, H 3.08, N 30.57; found C 52.14, H 3.11, N 30.40. M.p. (uncorrected): 288–289 °C (dec.). MS (EI<sup>+</sup>, 70 keV, >5%):  $m/z = 229.2$  [M + H]<sup>+</sup>.  $^1\text{H}$  NMR ([D<sub>6</sub>]DMSO, 400.18 MHz, TMS):  $\delta = 3.46$  (s, 3 H, CH<sub>3</sub>), AA'BB' spin system: 8.04, 7.97 (m, 4 H, arom-H) ppm.  $^{13}\text{C}\{^1\text{H}\}$  NMR ([D<sub>6</sub>]DMSO, 100.52 MHz, TMS):  $\delta = 165.2$  (2 C, C-2/C-9), 153.8 (1 C, C-1), 135.7 (2 C, C-5/C-6), 131.1 (2 C, C-3/C-8), 124.4 (2 C, C-4/C-7), 40.6 (1 C, CH<sub>3</sub>) ppm. Raman:  $\tilde{\nu}$  (rel. int.) = 3083 (18), 3068 (25), 3056 (22), 3030 (11), 2969 (24), 2851 (4), 1792 (100), 1765 (28), 1742 (14), 1720 (7), 1610 (31), 1531 (52), 1467 (12), 1437 (10), 1404 (7), 1369 (12), 1353 (15), 1302 (10), 1207 (14), 1175 (67), 1156 (23), 1085 (6), 1036 (41), 1010 (38), 886 (13), 841 (10), 797 (6), 718 (10), 674 (71), 578 (19), 460 (3), 378 (7), 362 (19), 332 (5), 272 (12), 253 (32), 193 (10), 171 (16), 89 (3) cm<sup>-1</sup>.

**Synthesis of 5-Amino-2-methyltetrazole (**5**)**

**Method 1:** Crystalline material of **5** was obtained by slow cooling of a saturated benzene/hexane solution, as described previously, in a maximum yield of around 18%.<sup>[9]</sup> Crystals for X-ray structure determination were obtained by vacuum sublimation.

**Method 2:** Tetrazole **2** (11.478 g, 50.08 mmol) was dissolved in ethanol (100 mL) and treated with an excess of hydrazine monohydrate (9 mL, 185.48 mmol) to form a slightly yellow solution, which was stirred and heated at reflux for 2 h. At this point glacial acetic acid (5 mL) was added to the reaction mixture, which was heated at reflux for a further 1 h. Coarse crystals of **5** formed upon slow cooling to room temperature, which were filtered, washed with cold acetone and dried under vacuum. A second crop of the product could be obtained by concentrating the mother liquor (combined yield: 4.173 g, 84%).  $\text{C}_2\text{H}_5\text{N}_5$  (99.06): calcd. C 24.24, H 5.08, N 70.67; found C 24.19, H 4.82, N 70.60. DSC (5 °C min<sup>-1</sup> °C, onset): 102 (m.p.). MS (EI<sup>+</sup>, 70 eV, >5%):  $m/z$  (%) = 113 (8), 99 (8) [M]<sup>+</sup>, 71 (13), 57 (7), 43 (24), 42 (45), 28 (35), 18 (100), 15 (18).  $^1\text{H}$  NMR ([D<sub>6</sub>]DMSO, 400.18 MHz, TMS):  $\delta = 5.92$  (s, 2 H, NH<sub>2</sub>), 4.06 (s, 3 H, CH<sub>3</sub>) ppm.  $^{13}\text{C}\{^1\text{H}\}$  NMR ([D<sub>6</sub>]DMSO, 100.52 MHz, TMS):  $\delta = 167.7$  (C<sub>arom</sub>), 39.4 (CH<sub>3</sub>) ppm.  $^{15}\text{N}\{^1\text{H}\}$  NMR ([D<sub>6</sub>]DMSO, 40.51 MHz, MeNO<sub>2</sub>):  $\delta = -6.5$  (1 N, N-3), -83.3 (1 N, N-

4), -115.6 (1 N, N-1), -115.7 (1 N, N-2), -339.7 (1 N, NH<sub>2</sub>) ppm. Raman:  $\tilde{\nu}$  (rel. int.) = 3213 (19), 3025 (21), 2960 (90), 1646 (18), 1544 (53), 1449 (26), 1375 (76), 1314 (17), 1200 (40), 1127 (17), 1084 (85), 1056 (30), 1016 (73), 805 (17), 649 (100), 473 (48), 319 (42), 159 (37) cm<sup>-1</sup>. IR (KBr):  $\tilde{\nu}$  = 3385 (s), 3307 (s), 3217 (s), 3083 (w), 2959 (w), 2758 (w), 1635 (s), 1553 (s), 1448 (m), 1420 (w), 1409 (m), 1376 (m), 1314 (m), 1204 (s), 1124 (w), 1084 (w), 1054 (w), 1015 (m), 808 (m), 757 (m), 649 (s), 488 (m) cm<sup>-1</sup>.

#### Synthesis of 2-Methyl-5-aminotetrazol-4-ium Perchlorate (7):

Tetrazole **5** (0.25 g, 2.52 mmol) was dissolved in the minimum amount of 72% concentrated perchloric acid. The reaction mixture was layered with diethyl ether and stored in a fridge overnight yielding colourless plates of the product, which were filtered, washed with diethyl ether and allowed to air-dry. No further purification was necessary. Single crystals of the compound suitable for X-ray analysis were obtained by ether diffusion into a concentrated methanolic solution (0.39 g, 77%). C<sub>2</sub>H<sub>6</sub>ClN<sub>5</sub>O<sub>4</sub> (199.01): calcd. C 12.02, H 3.05, N 35.12, Cl 17.57; found C 12.04, H 3.03, N 35.09, Cl 17.98, DSC (5 °C min<sup>-1</sup> °C, onset): 125 (m.p.), 196 (dec.). MS (FAB<sup>+</sup>, xenon, 6 keV, *m*-NBA matrix): *m/z* = 100.0 [cation]<sup>+</sup>. <sup>1</sup>H NMR ([D<sub>6</sub>]DMSO, 400.18 MHz, TMS):  $\delta$  = 8.67 (s, 2 H, NH<sub>2</sub>), 7.51 (s, 1 H, NH), 3.97 (s, 3 H, CH<sub>3</sub>) ppm. <sup>13</sup>C{<sup>1</sup>H} NMR ([D<sub>6</sub>]DMSO, 100.63 MHz, TMS):  $\delta$  = 166.8 (1 C, C-ring), 40.7 (1 C, CH<sub>3</sub>) ppm. <sup>15</sup>N NMR ([D<sub>6</sub>]DMSO, 40.55 MHz, MeNO<sub>2</sub>):  $\delta$  = -8.8 (q, *J* = 1.33 Hz, 1 N, N-3), -90.0 (s, 1 N, N-4) -113.4 (s, 1 N, N-1), -114.2 (s, 1 N, N-2), -340.1 (s, 1 N, NH<sub>2</sub>) ppm. Raman:  $\tilde{\nu}$  (rel. int.) = 3198 (5), 3046 (8), 2972 (22), 1686 (7), 1492 (7), 1442 (22), 1411 (13), 1385 (19), 1182 (9), 1091 (21), 1024 (27), 926 (100), 803 (14), 651 (25), 637 (21), 623 (16), 479 (19), 468 (20), 453 (22), 321 (19), 224 (9) cm<sup>-1</sup>. IR (KBr):  $\tilde{\nu}$  = 3287 (s), 3254 (s), 3183 (s), 3097 (s), 3025 (m), 2756 (m), 2480 (w), 2351 (w), 2319 (w), 2139 (w), 2030 (w), 1661 (vs), 1586 (m), 1575 (w), 1442 (w), 1408 (w), 1391 (w), 1333 (w), 1180 (m), 1145 (s), 1109 (vs), 1089 (vs), 1018 (m), 940 (w), 923 (w), 803 (w), 732 (w), 696 (m), 672 (w), 647 (m), 637 (m), 626 (s), 481 (w) cm<sup>-1</sup>.

**Synthesis of 5-Amino-2-methyltetrazol-4-ium Nitrate (8):** Solid crystalline **5** (0.100 g, 1.0 mmol) was dissolved in a minimum of concentrated (65%) nitric acid. The clear, colourless reaction mixture was stirred until all **5** had dissolved. The solution was then cooled to 4 °C overnight to yield the formation of clear colourless crystals suitable for X-ray analysis, which were filtered off cold and washed until dry and acid-free with diethyl ether. No further purification was necessary (0.073 g, 73%). C<sub>2</sub>H<sub>6</sub>N<sub>6</sub>O<sub>3</sub> (162.05): calcd. C 14.81, H 3.73, N 51.84; found C 14.70, H 3.68, N 51.26. DSC (5 °C min<sup>-1</sup> °C, onset): 123.2 (m.p.), 161.4 (dec.). MS (FAB<sup>+</sup>, xenon, 6 keV, *m*-NBA matrix): *m/z* = 100.0 [2MAT]<sup>+</sup>. <sup>1</sup>H NMR ([D<sub>6</sub>]DMSO, 400.18 MHz, TMS):  $\delta$  = 8.50 (s, 3 H, NH + NH<sub>2</sub>), 4.01 (s, 3 H, CH<sub>3</sub>) ppm. <sup>13</sup>C{<sup>1</sup>H} NMR ([D<sub>6</sub>]DMSO, 100.63 MHz, TMS):  $\delta$  = 167.2 (1 C, C-ring), 38.9 (1 C, CH<sub>3</sub>) ppm. <sup>14</sup>N{<sup>1</sup>H} NMR ([D<sub>6</sub>]DMSO, 40.55 MHz, MeNO<sub>2</sub>):  $\delta$  = -14 (1 N, NO<sub>3</sub><sup>-</sup>), -111 (2 N, N-1/N-2) ppm. <sup>15</sup>N NMR ([D<sub>6</sub>]DMSO, 40.55 MHz, MeNO<sub>2</sub>):  $\delta$  = -6.9 (q, *J* = 1.30 Hz, 1 N, N-3), -15.1 (s, 1 N, NO<sub>3</sub><sup>-</sup>), -84.4 (s, 1 N, N-4) -114.4 (s, 1 N, N-1), -114.9 (s, 1 N, N-2), -339.5 (s, 1 N, NH<sub>2</sub>) ppm. Raman:  $\tilde{\nu}$  (rel. int.) = 3192 (3), 3049 (11), 3039 (9), 2968 (30), 1663 (9), 1437 (21), 1383 (27), 1297 (5), 1189 (11), 1086 (18), 1043 (100), 1010 (18), 789 (15), 728 (11), 713 (9), 649 (33), 480 (14), 321 (23), 212 (9), 141 (22) cm<sup>-1</sup>. IR (KBr):  $\tilde{\nu}$  = 3383 (m), 3249 (m), 3184 (m), 3049 (w), 2925 (w), 2853 (w), 2637 (w), 2426 (w), 1677 (s), 1430 (m), 1384 (s), 1308 (m), 1187 (w), 1073 (m), 1041 (m), 1010 (m), 953 (w), 823 (m), 787 (m), 726 (m), 647 (m), 575 (m), 478 (w) cm<sup>-1</sup>.

**Synthesis of 5-Amino-1,3-dimethyltetrazol-3-ium Perchlorate (9):** A solution of silver perchlorate (2.04 g, 9.84 mmol) in methanol

(20 mL) was added to a solution of **6** (2.37 g, 9.83 mmol) in methanol (20 mL) and stirred under light exclusion for 1 h. The precipitated silver iodide was then filtered and washed with methanol. After removing the solvent, the colourless residue was dissolved in a small amount of methanol and recrystallized overnight in an ether chamber. After filtering the colourless solid, this was dried on air (1.63 g, 78%). C<sub>3</sub>H<sub>8</sub>ClN<sub>5</sub>O<sub>4</sub> (213.02): calcd. C 16.89, H 3.78, N 32.86, Cl 16.41; found C 16.91, H 3.86, N 32.72, Cl 17.73. DSC (5 °C min<sup>-1</sup> °C, onset): 132.3 (m.p.), 285.1 (dec.). MS (FAB<sup>+</sup>, xenon, 6 keV, *m*-NBA matrix): *m/z* = 114.2 [cation]<sup>+</sup>. <sup>1</sup>H NMR ([D<sub>6</sub>]DMSO, 499.78 MHz, TMS):  $\delta$  = 8.23 (s, 2 H, NH<sub>2</sub>), 4.30 (s, 3 H, 3-CH<sub>3</sub>), 3.87 (s, 3 H, 2-CH<sub>3</sub>) ppm. <sup>13</sup>C{<sup>1</sup>H} NMR ([D<sub>6</sub>]DMSO, 100.52 MHz, TMS):  $\delta$  = 158.09 (1 C, C-ring), 42.54 (1 C, 3-CH<sub>3</sub>), 34.18 (1 C, 2-CH<sub>3</sub>) ppm. <sup>35</sup>Cl NMR ([D<sub>6</sub>]DMSO, 39.21 MHz, NaCl):  $\delta$  = 1.01 (ClO<sub>4</sub>). <sup>15</sup>N{<sup>1</sup>H} NMR ([D<sub>6</sub>]DMSO, 40.55 MHz, MeNO<sub>2</sub>):  $\delta$  = -31.43 (1 N, N-4), -108.71 (1 N, N-3), -110.76 (1 N, N-2), -180.26 (1 N, N-5), -327.01 (1 N, NH<sub>2</sub>) ppm. <sup>15</sup>N NMR ([D<sub>6</sub>]DMSO, 40.51 MHz, MeNO<sub>2</sub>):  $\delta$  = -32.04 (q, <sup>2</sup>*J* = 2.79 Hz, 1 N, N-4), -109.32 (q, <sup>3</sup>*J* = 1.86 Hz, 1 N, N-3), -111.30 (q, <sup>2</sup>*J* = 2.79 Hz, 1 N, N-2), -180.84 (q, <sup>3</sup>*J* = 1.86 Hz, 1 N, N-5), -327.18 (t, <sup>1</sup>*J* = 89.51 Hz, 1 N, NH<sub>2</sub>) ppm. Raman:  $\tilde{\nu}$  (rel. int.) = 3427 (1), 3238 (2), 3053 (10), 3025 (11), 2966 (46), 2818 (2), 1666 (9), 1595 (4), 1500 (6), 1442 (13), 1416 (29), 1396 (9), 1294 (5), 1261 (15), 1118 (8), 1076 (12), 1015 (6), 936 (100), 854 (21), 820 (2), 680 (11), 634 (33), 529 (4), 464 (22), 318 (21), 290 (8), 238 (10), 194 (4), 84 (1) cm<sup>-1</sup>. IR (KBr):  $\tilde{\nu}$  = 3434 (m), 3308 (m), 3220 (m), 3217 (m), 3047 (s), 2946 (m), 2840 (w), 2767 (w), 2704 (w), 2657 (w), 2501 (w), 2439 (vw), 2184 (w), 2122 (w), 2024 (w), 1923 (w), 1864 (w), 1666 (vs), 1593 (s), 1566 (w), 1497 (w), 1468 (m), 1430 (m), 1384 (w), 1363 (m), 1290 (m), 1251 (m), 1144 (s), 1120 (s), 1088 (s), 1013 (m), 940 (w), 852 (m), 726 (w), 674 (w), 626 (m), 568 (w) cm<sup>-1</sup>.

#### Synthesis of 5-Amino-1,3-dimethyltetrazol-3-ium Nitrate (10):

A solution of silver nitrate (0.60 g, 3.53 mmol) in methanol (5 mL) was added with stirring to a solution of **6** (0.85 g, 3.53 mmol) in methanol (10 mL). Under exclusion of light the solution was stirred at room temperature for 50 min and then filtered. After evaporating the solvent the slightly brown residue was dissolved in the minimum amount of methanol and crystallized overnight in an ether chamber. The colourless precipitate was then filtered under vacuum and dried in air (0.52 g, 79%). C<sub>3</sub>H<sub>8</sub>N<sub>6</sub>O<sub>3</sub> (176.06): calcd. C 20.46, H 4.58, N 47.71; found C 20.38, H 4.48, N 47.66. DSC (5 °C min<sup>-1</sup> °C, onset): 150.1 (m.p.), 198.5 (dec.). MS (FAB<sup>+</sup>, xenon, 6 keV, *m*-NBA matrix): *m/z* = 114.2 [cation]<sup>+</sup>. <sup>1</sup>H NMR ([D<sub>6</sub>]DMSO, 399.78 MHz, TMS):  $\delta$  = 8.27 (s, 2 H, NH<sub>2</sub>), 4.30 (s, 3 H, 3-CH<sub>3</sub>), 3.87 (s, 3 H, 2-CH<sub>3</sub>) ppm. <sup>13</sup>C{<sup>1</sup>H} NMR ([D<sub>6</sub>]DMSO, 100.52 MHz, TMS):  $\delta$  = 158.60 (1 C, C-ring), 43.04 (1 C, 3-CH<sub>3</sub>), 34.64 (1 C, 2-CH<sub>3</sub>) ppm. <sup>14</sup>N NMR ([D<sub>6</sub>]DMSO, 28.88 MHz, MeNO<sub>2</sub>):  $\delta$  = 3.82 (1 N, NO<sub>3</sub><sup>-</sup>) ppm. <sup>15</sup>N NMR ([D<sub>6</sub>]DMSO, 40.51 MHz, MeNO<sub>2</sub>):  $\delta$  = -4.54 (s, 1 N, NO<sub>3</sub>), -32.63 (q, <sup>2</sup>*J* = 2.32 Hz, 1 N, N-4), -109.61 (q, <sup>3</sup>*J* = 1.86 Hz, 1 N, N-3), -111.08 (q, <sup>2</sup>*J* = 2.79 Hz, 1 N, N-2), -181.18 (m, 1 N, N-5), -326.05 (s, <sup>1</sup>*J* = 89.5 Hz, 1 N, NH<sub>2</sub>) ppm. Raman:  $\tilde{\nu}$  (rel. int.) = 3028 (7), 2994 (5), 2965 (29), 1660 (5), 1593 (5), 1444 (10), 1415 (18), 1294 (5), 1257 (12), 1126 (5), 1077 (13), 1049 (100), 1014 (7), 852 (17), 714 (11), 678 (9), 632 (19), 534 (5), 363 (4), 328 (15), 300 (6) 236 (7), 207 (6), 105 (1), 85 (1) cm<sup>-1</sup>. IR (KBr):  $\tilde{\nu}$  = 3307 (w), 3217 (m), 3045 (m), 2767 (w), 2703 (w), 2657 (w), 2499 (w), 2426 (w), 2395 (w), 2184 (w), 2122 (w), 1659 (s), 1593 (m), 1384 (vs), 1289 (w), 1250 (m), 1116 (m), 1081 (w), 1014 (w), 851 (w), 825 (w), 725 (w), 674 (w), 627 (w), 569 (w), 365 (w), 332 (w) cm<sup>-1</sup>.

**Synthesis of 5-Amino-1,3-dimethyltetrazol-3-ium Azide (11):** The salt **6** (2.13 g, 8.85 mmol) was added to a suspension of freshly prepared silver azide (1.50 g, 10.01 mmol) in methanol (50 mL).

The reaction mixture was stirred under the exclusion of light at room temperature for around 1.5 h and then filtered. After the solvent was evaporated the colourless solid was dried under high vacuum (1.110 g, 81%). C<sub>3</sub>H<sub>8</sub>N<sub>8</sub> (156.09): calcd. C 23.06, H 5.16, N 71.77; found C 23.04, H 4.94, N 71.47. DSC [5 °C min<sup>-1</sup> (°C, onset): 170.8 (m.p.), ca. 282 (dec.). M.p. 171.3–172.7 °C (Büchi, uncorrected). MS (FAB<sup>+</sup>, xenon, 6 keV, *m*-NBA matrix): *m/z* = 114.1 [cation]<sup>+</sup>. <sup>1</sup>H NMR ([D<sub>6</sub>]DMSO, 399.78 MHz, TMS): δ = 8.47 (s, 2 H, NH<sub>2</sub>), 4.30 (s, 3 H, 3-CH<sub>3</sub>), 3.88 (s, 3 H, 2-CH<sub>3</sub>) ppm. <sup>13</sup>C{<sup>1</sup>H} NMR ([D<sub>6</sub>]DMSO, 100.52 MHz, TMS): δ = 158.15 (1 C, C-ring), 42.49 (1 C, 3-CH<sub>3</sub>), 34.13 (1 C, 2-CH<sub>3</sub>) ppm. <sup>14</sup>N NMR ([D<sub>6</sub>]DMSO, 28.88 MHz, MeNO<sub>2</sub>): δ = -133 (1 N, N-N-N, N<sub>3</sub><sup>-</sup>), -277 (2 N, N-N-N, N<sub>3</sub><sup>-</sup>) ppm. <sup>15</sup>N NMR ([D<sub>6</sub>]DMSO, 40.51 MHz, MeNO<sub>2</sub>): δ = -33.14 (q, <sup>2</sup>*J* = 2.60 Hz, 1 N, N-4), -113.22 (q, <sup>3</sup>*J* = 2.53 Hz, 1 N, N-3), -113.40 (q, <sup>2</sup>*J* = 2.91 Hz, 1 N, N-2), -135.15 (1 N, N-N-N, N<sub>3</sub><sup>-</sup>), -188.99 (q, <sup>3</sup>*J* = 1.97 Hz, 1 N, N-5), -285 (2 N, N-N-N, N<sub>3</sub><sup>-</sup>), -327.57 (t, <sup>1</sup>*J* = 86.25 Hz, 1 N, NH<sub>2</sub>) ppm. Raman:  $\tilde{\nu}$  (rel. int.) = 3038 (9), 2957 (36), 2809 (2), 1664 (10), 1609 (4), 1500 (5), 1436 (10), 1412 (7), 1388 (9), 1341 (62), 1301 (5), 1266 (12), 1135 (5), 1076 (16), 1019 (4), 858 (26), 814 (2), 727 (2), 681 (7), 639 (33), 624 (5), 599 (2), 544 (12), 439 (2), 341 (13), 293 (12), 236 (8), 158 (8), 123 (2) cm<sup>-1</sup>. IR (KBr):  $\tilde{\nu}$  = 3359 (m), 3334 (m), 3253 (m), 3067 (s), 2926 (m), 2790 (m), 2731 (m), 2519 (w), 2461 (w), 2206 (vw), 2054 (vs), 2042 (vs), 1669 (s), 1604 (s), 1536 (w), 1495 (w), 1460 (w), 1446 (w), 1385 (m), 1370 (m), 1317 (vw), 1297 (w), 1264 (m), 1131 (m), 1089 (m), 1075 (m), 1018 (w), 856 (m), 727 (m), 680 (m), 645 (w), 636 (w), 622 (w), 571 (m), 543 (m) cm<sup>-1</sup>.

### Synthesis of 5-Amino-1,3-dimethyltetrazol-3-ium Dinitramide (12)

**Method 1:** The salt **6** (1.04 g, 4.33 mmol) was added to a suspension of silver bis(pyridine) dinitramide (1.60 g, 4.30 mmol) in methanol (15 mL). Under the exclusion of light the suspension was stirred at room temperature for 2 h and then filtered. After removing the solvent under vacuum the colourless crude solid was dissolved in a small amount of methanol and crystallized overnight in an ether chamber. As no precipitation was observed the sample was left to evaporate and an oily green-yellow liquor formed. Crystallization was induced by scratching with a glass stirrer on the sides of the glass vessel. The colourless solid was then scratched out, filtered and washed with diethyl ether (0.70 g, 73.37%).

**Method 2:** In the first synthesis step the nitrate salt (**10**) was generated by the addition of **6** (5.08 g, 21.08 mmol) to a solution of silver nitrate (3.54 g, 20.87 mmol) in methanol (80 mL) followed by stirring at room temperature for about 2 h. After filtration, the solvent was evaporated and the colourless residue was dissolved in a minimum amount of methanol and diethyl ether was allowed to diffuse into the methanol solution overnight yielding clear colourless quadrangular crystals, which were identified as 5-amino-1,3-dimethyltetrazolium nitrate by measuring the melting point (150.8 °C–152.9 °C). In the second step **10** (0.96 g, 5.45 mmol) was dissolved in ethanol (40 mL) and potassium dinitramide (0.79 g, 5.46 mmol) was added. The reaction mixture was heated at 80 °C for 4 h and then filtered whilst hot. After evaporating the solvent the yellow oily residue was dried under high vacuum to yield an oil. Crystallization was induced by scratching with a glass stirrer on the sides of the flask yielding a slightly yellow product (1.12 g, 93%). C<sub>3</sub>H<sub>8</sub>N<sub>8</sub>O<sub>4</sub> (220.07): calcd. C 16.37, H 3.66, N 50.90; found C 16.20, H 3.70, N 50.83. DSC (5 °C min<sup>-1</sup> °C, onset): 57.9 (m.p.), 168.4 (dec.). MS (FAB<sup>+</sup>, xenon, 6 keV, *m*-NBA matrix): *m/z* = 114.1 [cation]<sup>+</sup>; (FAB<sup>-</sup>, xenon, 6 keV, *m*-NBA matrix): *m/z* = 106.0 [Anion]<sup>-</sup>. <sup>1</sup>H NMR ([D<sub>6</sub>]DMSO, 399.78 MHz, TMS): δ = 8.21 (s, 2 H, NH<sub>2</sub>), 4.24 (s, 3 H, 3-CH<sub>3</sub>), 3.86 (s, 3 H, 2-CH<sub>3</sub>) ppm. <sup>13</sup>C{<sup>1</sup>H} NMR ([D<sub>6</sub>]DMSO, 100.52 MHz, TMS): δ = 158.58 (1 C, C-ring),

42.93 (1 C, 3-CH<sub>3</sub>), 34.57 (1 C, 2-CH<sub>3</sub>) ppm. <sup>14</sup>N NMR ([D<sub>6</sub>]DMSO, 28.88 MHz, MeNO<sub>2</sub>): δ = -10 (2 N, NO<sub>2</sub>) ppm. <sup>15</sup>N{<sup>1</sup>H} NMR ([D<sub>6</sub>]DMSO, 40.51 MHz, MeNO<sub>2</sub>): δ = -11.28 (2 N, NO<sub>2</sub>), -32.24 (1 N, N-4), -57.24 [1 N, N(NO<sub>2</sub>)<sub>2</sub>], -109.38 (1 N, N-3), -111.12 (1 N, N-2), -181.02 (1 N, N-5), -326.81 (1 N, NH<sub>2</sub>) ppm. <sup>15</sup>N NMR ([D<sub>6</sub>]DMSO, 40.51 MHz, MeNO<sub>2</sub>): δ = -11.29 (s, 2 N, NO<sub>2</sub>), -32.29 (1 N, N-4), -57.22 [1 N, N(NO<sub>2</sub>)<sub>2</sub>], -109.43 (q, <sup>3</sup>*J* = 1.86 Hz, 1 N, N-3), -111.18 (q, <sup>2</sup>*J* = 2.79 Hz, 1 N, N-2), -181.06 (1 N, N-5), -326.79 (s, 1 N, NH<sub>2</sub>) ppm. Raman:  $\tilde{\nu}$  (rel. int.) = 3238 (5), 3169 (5), 3144 (5), 3053 (11), 3032 (12), 2964 (28), 2829 (5), 2676 (5), 2563 (7), 2510 (8), 2467 (8), 2434 (8), 2336 (8), 2294 (8), 2283 (8), 2245 (8), 2204 (9), 2184 (8), 2156 (9), 2135 (9), 2060 (9), 1870 (14), 1820 (15), 1700 (15), 1670 (22), 1602 (16), 1561 (16), 1519 (25), 1496 (25), 1457 (28), 1439 (31), 1421 (27), 1394 (25), 1324 (100), 1254 (22), 1176 (16), 1115 (13), 1082 (20), 1052 (19), 1019 (14), 964 (13), 946 (14), 856 (29), 825 (28), 761 (7), 706 (5), 680 (11), 632 (37), 531 (5), 480 (26), 418 (5), 388 (4), 325 (16), 300 (16), 246 (10), 203 (7) cm<sup>-1</sup>. IR (KBr):  $\tilde{\nu}$  = 3399 (m), 3345 (m), 3301 (m), 3239 (m), 3182 (m), 1668 (s), 1600 (w), 1515 (s), 1430 (m), 1384 (m), 1324 (w), 1295 (w), 1253 (w), 1186 (vs), 1117 (w), 1082 (w), 1011 (m), 854 (m), 824 (w), 760 (m), 726 (m), 676 (w), 629 (w), 564 (w), 478 (w) cm<sup>-1</sup>.

**Supporting Information** (see also the footnote on the first page of this article): Tables containing extensive X-ray data and the results of calculations, NMR analysis and “flame tests”.

### Acknowledgments

Financial support of this work by the Ludwig-Maximilians-Universität München (LMU), the Fonds der Chemischen Industrie (FCI), the European Research Office (ERO) of the U.S. Army Research Laboratory (ARL) and Armament Research, Development and Engineering Center (ARDEC) under contract nos. N 62558-05-C-0027, R&D 1284-CH-01, R&D 1285-CH-01, 9939-AN-01 and W911NF-07-1-0569 and the Bundeswehr Research Institute for Materials, Explosives, Fuels and Lubricants (WIWEB) under contract nos. E/E210/4D004/X5143 and E/E210/7D002/4F088 is gratefully acknowledged. The authors acknowledge collaborations with Dr. M. Krupka (OZM Research, Czech Republic) in the development of new testing and evaluation methods for energetic materials and with Dr. M. Sucasca (Brodarski Institute, Croatia) in the development of new computational codes to predict the detonation parameters of high-nitrogen explosives. We are indebted to and thank Dr. Betsy M. Rice (ARL, Aberdeen, Proving Ground, MD) for many helpful and inspired discussions and support of our work.

- [1] U. Bemm, H. Ostmark, *Acta Crystallogr., Sect. C* **1998**, *54*, 1997–1999.
- [2] H. H. Cady, A. C. Larson, *Acta Crystallogr.* **1965**, *18*, 485–496.
- [3] a) C. Ye, J. Xiao, B. Twamley, J. M. Shreeve, *Chem. Commun.* **2005**, *21*, 2750–2752; b) R. P. Singh, R. D. Verma, D. T. Meshri, J. M. Shreeve, *Angew. Chem. Int. Ed.* **2006**, *45*, 3584–3601, and references therein.
- [4] a) Y. Huang, H. Gao, B. Twamley, J. M. Shreeve, *Eur. J. Inorg. Chem.* **2007**, *14*, 2025–2030; b) H. Xue, H. Gao, B. Twamley, J. M. Shreeve, *Eur. J. Inorg. Chem.* **2006**, *15*, 2959–2965; c) H. Xue, Y. Gao, B. Twamley, J. M. Shreeve, *Chem. Mater.* **2005**, *17*, 191–198; d) H. Xue, B. Twamley, J. M. Shreeve, *J. Mater. Chem.* **2005**, *15*, 3459–3465.
- [5] a) Y. Gao, C. Ye, B. Twamley, J. M. Shreeve, *Chem. Eur. J.* **2006**, *12*, 9010–9018; b) H. Gao, R. Wang, B. Twamley, M. A. Hiskey, J. M. Shreeve, *Chem. Commun.* **2006**, 4007–4009; c) R. Wang, H. Gao, C. Ye, J. M. Shreeve, *Chem. Mater.* **2007**, *19*,

- 144–152; d) R. Wang, H. Gao, C. Ye, B. Twamley, J. M. Shreeve, *Inorg. Chem.* **2007**, *46*, 932–938; e) H. Gao, C. Ye, O. D. Gupta, J.-C. Xiao, M. A. Hiskey, B. Twamley, J. M. Shreeve, *Chem. Eur. J.* **2007**, *13*, 3853–3860; f) Y. Guo, H. Gao, B. Twamley, J. M. Shreeve, *Adv. Mater.* **2007**, *19*, 2884–2888.
- [6] a) Z. Zeng, H. Gao, B. Twamley, J. M. Shreeve, *J. Mater. Chem.* **2007**, *17*, 3819–3826; b) C. Ye, H. Gao, J. M. Shreeve, *J. Fluorine Chem.* **2007**, *128*, 1410–1415; c) C. Ye, G. L. Gard, R. W. Winter, R. G. Syvret, B. Twamley, J. M. Shreeve, *Org. Lett.* **2007**, *9*, 3841–3844; d) C. Ye, H. Gao, B. Twamley, J. M. Shreeve, *New J. Chem.* **2008**, *32*, 317–322; e) H. Gao, Z. Zeng, B. Twamley, J. M. Shreeve, *Chem. Eur. J.* **2008**, *14*, 1282–1290; f) H. Gao, Y. Huang, B. Twamley, C. Ye, J. M. Shreeve, *Chem. Sus. Chem.* **2008**, *2*, 222–227; g) H. Gao, Y. Huang, C. Ye, B. Twamley, J. M. Shreeve, *Chem. Eur. J.* **2008**, *14*, 5596–5603; h) Y. Huang, H. Gao, B. Twamley, J. M. Shreeve, *Eur. J. Inorg. Chem.* **2008**, 2560–2568; i) Y.-H. Joo, B. Twamley, S. Garg, J. M. Shreeve, *Angew. Chem. Int. Ed.* **2008**, ASAP.
- [7] a) A. Hammerl, M. A. Hiskey, G. Holl, T. M. Klapötke, K. Polborn, J. Stierstorfer, J. J. Weigand, *Chem. Mater.* **2005**, *17*, 3784–3793; b) J. Geith, T. M. Klapötke, J. J. Weigand, G. Holl, *Propellants Explos. Pyrotech.* **2004**, *29*, 3–8; c) M. von Denffer, T. M. Klapötke, G. Kramer, G. Spiess, J. M. Welch, G. Heeb, *Propellants Explos. Pyrotech.* **2005**, *30*, 191–195.
- [8] K. Karaghiosoff, T. M. Klapötke, P. Mayer, C. Miró Sabaté, A. Penger, J. M. Welch, *Inorg. Chem.* **2008**, *47*, 1007–1019.
- [9] R. A. Henry, W. G. Finnegan, E. Lieber, *J. Am. Chem. Soc.* **1954**, *76*, 2894–2898.
- [10] a) J. Miller, DE 2506775, **1975**; b) Dynamit Nobel A.G., GB 1570320, **1980**.
- [11] J. C. Gálvez-Ruiz, G. Holl, K. Karaghiosoff, T. M. Klapötke, K. Löhnitz, P. Mayer, H. Nöth, K. Polborn, C. J. Rohbogner, M. Suter, J. J. Weigand, *Inorg. Chem.* **2005**, *44*, 4237–4253.
- [12] T. M. Klapötke, C. Miró Sabaté, M. Rusan, *Z. Anorg. Allg. Chem.* **2008**, *634*, 688–695.
- [13] A. Bigotto, R. Klingendrath, *Spectrochim. Acta Part A* **1990**, *46*, 1683–1692.
- [14] a) K. Williamson, P. Li, J. P. Devlin, *J. Chem. Phys.* **1968**, *48*, 3891–3896; b) J. R. Fernandes, S. Ganguly, C. N. R. Rao, *Spectrochim. Acta Part A* **1979**, *35*, 1013–1019.
- [15] a) H. Cohn, *J. Chem. Soc.* **1952**, 4282–4284; b) P. Redlich, J. Holt, T. Biegeleisen, *J. Am. Chem. Soc.* **1944**, *66*, 13–16; c) H. Grothe, H. Willner, *Angew. Chem. Int. Ed. Engl.* **1996**, *35*, 768.
- [16] U. Müller, *Struct. Bonding (Berlin)* **1974**, *14*, 141–145.
- [17] K. O. Christe, W. W. Wilson, M. A. Petrie, H. H. Michels, J. C. Bottaro, R. Gilardi, *Inorg. Chem.* **1996**, *35*, 5068–5071.
- [18] N. B. Colthup, L. H. Daly, S. E. Wiberley, *Introduction to Infra-red, Raman Spectroscopy*; Academic Press, Boston, **1990**.
- [19] C. Darwich, T. M. Klapötke, C. Miró Sabaté, *Chem. Eur. J.* **2008**, *14*, 5756–5771.
- [20] a) C. Darwich, K. Karaghiosoff, T. M. Klapötke, C. Miró Sabaté, *Z. Anorg. Allg. Chem.* **2008**, *634*, 61–68; b) A. Garrone, R. Fruttero, C. Tironi, A. Gasco, *J. Chem. Soc. Perkin Trans. 2* **1989**, *12*, 1941–1945.
- [21] *ABSPACK, CrysAlis CCD, CrysAlis RED*, Versions 1.171, Oxford Diffraction Ltd., Abingdon, England, **2006**.
- [22] *SIR-92, A Program for Crystal Structure Solution*: A. Altomare, G. Casciarano, C. Giacovazzo, A. Guagliardi, *J. Appl. Crystallogr.* **1993**, *26*, 343.
- [23] G. M. Sheldrick, *SHELXL-97, Program for the Refinement of Crystal Structures*, University of Göttingen, Germany, **1997**.
- [24] *WinGX Suite for Small Molecule Single-Crystal Crystallography*: L. J. Farrugia, *J. Appl. Crystallogr.* **1999**, *32*, 837–838.
- [25] A. L. Spek, *PLATON, A Multipurpose Crystallographic Tool*, Utrecht University, Utrecht, The Netherlands, **1999**.
- [26] J. H. Bryden, *Acta Crystallogr.* **1956**, *9*, 874–878.
- [27] The N–N and N=N values are from: *International Tables for X-ray Crystallography*, Kluwer Academic Publishers, Dordrecht, The Netherlands, **1992**, vol. C.
- [28] T. M. Klapötke, P. Mayer, A. Schulz, J. J. Weigand, *J. Am. Chem. Soc.* **2005**, *127*, 2032–2033.
- [29] A. H. Pakiari, K. Eskandari, *THEOCHEM* **2007**, *806*, 1–7.
- [30] *NATO Standardization Agreement (STANAG) on Explosives, Impact Sensitivity Tests*, No. 4489, 1st ed., Sept. 17, **1999**.
- [31] *WIWEB-Standardarbeitsanweisung 4-5.1.02, Ermittlung der Explosionsgefährlichkeit, hier der Schlagempfindlichkeit mit dem Fallhammer*, Nov. 8, **2002**.
- [32] <http://www.bam.de>.
- [33] *NATO Standardization Agreement (STANAG) on Explosives, Friction Sensitivity Tests*, No. 4487, 1st ed., Aug. 22, **2002**.
- [34] H. D. B. Jenkins, D. Tudela, L. Glasser, *Inorg. Chem.* **2002**, *41*, 2364–2367.
- [35] H. D. B. Jenkins, H. K. Roobottom, J. Passmore, L. Glasser, *Inorg. Chem.* **1999**, *38*, 3609–3620.
- [36] H. Gao, C. Ye, C. M. Piekarski, J. M. Shreeve, *J. Phys. Chem. C* **2007**, *111*, 10718–10731.
- [37] Calculation of the oxygen balance:  $\Omega(\%) = (O - 2C - H/2 - xAO)/1600/M$ , where  $M$  = molecular mass.
- [38] J. Koehler, R. Meyer, *Explosivstoffe*, 9th ed., Wiley-VCH, Weinheim, **1998**.
- [39] M. A. Hiskey, D. E. Chavez, D. L. Naud, S. F. Son, H. L. Berghout, C. A. Bolme, *Proc. Int. Pyrotech. Semin.* **2000**, *27*, 3–14.
- [40] Test methods according to the UN Recommendation on the Transport of Dangerous Goods, Manual of Tests, Criteria, 4th rev. ed., United Nations Publications, New York, **2003**.
- [41] a) Calculation of detonation parameters by the EXPLO5 computer program: M. Suceska, *Mater. Sci. Forum* **2004**, *465–466*, 325–330; b) M. Suceska, *Propellants Explos. Pyrotech.* **1991**, *16*, 197–202; c) M. Suceska, *Propellants Explos. Pyrotech.* **1999**, *24*, 280–285.
- [42] T. M. Klapötke, C. M. Rienäcker, *Propellants Explos. Pyrotech.* **2001**, *26*, 43–47.
- [43] <http://www.reichel-partner.de>.
- [44] a) S. Zeman, V. Pelikán, J. Majzlík, *Cent. Eur. J. Energ. Mater.* **2006**, *3*, 45–51; b) D. Skinner, D. Olson, A. Block-Bolten, *Propellants Explos. Pyrotech.* **1997**, *23*, 34–42.
- [45] <http://webbook.nist.gov>.
- [46] T. M. Klapötke, P. Mayer, C. Miró Sabaté, J. M. Welch, N. Wiegand, *Inorg. Chem.* **2008**, *47*, 6014–6027.
- [47] M. L. Hobbs, M. R. Baer, *Calibration of the BKW-EOS with a Large Product Species Data Base, Measured CJ Properties, Proceedings of the 10th International Symposium on Detonation*, ONR 33395-12, Boston, MA, July 12–16, **1993**, p. 409.
- [48] J. Akhavan, *The Chemistry of Explosives*, 2nd ed., RSC Paperbacks, Cambridge, **2004**.
- [49] T. M. Klapötke, C. Miró Sabaté, *Chem. Mater.* **2008**, *20*, 1750–1763.
- [50] M. J. Frisch, G. W. Trucks, H. B. Schlegel, G. E. Scuseria, M. A. Robb, J. R. Cheeseman, J. A. Montgomery Jr., T. Vreven, K. N. Kudin, J. C. Burant, J. M. Millam, S. S. Iyengar, J. Tomasi, V. Barone, B. Mennucci, M. Cossi, G. Scalmani, N. Rega, G. A. Petersson, H. Nakatsuji, M. Hada, M. Ehara, K. Toyota, R. Fukuda, J. Hasegawa, M. Ishida, T. Nakajima, Y. Honda, O. Kitao, H. Nakai, M. Klene, X. Li, J. E. Knox, H. P. Hratchian, J. B. Cross, C. Adamo, J. Jaramillo, R. Gomperts, R. E. Stratmann, O. Yazyev, A. J. Austin, R. Cammi, C. Pomelli, J. W. Ochterski, P. Y. Ayala, K. Morokuma, G. A. Voth, P. Salvador, J. J. Dannenberg, V. G. Zakrzewski, S. Dapprich, A. D. Daniels, M. C. Strain, O. Farkas, D. K. Malick, A. D. Rabuck, K. Raghavachari, J. B. Foresman, J. V. Ortiz, Q. Cui, A. G. Baboul, S. Clifford, J. Cioslowski, B. B. Stefanov, G. Liu, A. Liashenko, P. Piskorz, I. Komaromi, R. L. Martin, D. J. Fox, T. Keith, M. A. Al-Laham, C. Y. Peng, A. Nanayakkara, M. Challacombe, P. M. W. Gill, B. Johnson, W. Chen, M. W. Wong, C. Gonzalez, J. A. Pople, *Gaussian G03W, Gaussian 03, Revision A.1*, Gaussian Inc., Pittsburgh PA, **2003**.
- [51] J. A. Pople, R. Seeger, R. Krishnan, *Int. J. Quantum Chem. Symp.* **1977**, *11*, 149–163.

- [52] A. K. Rick, T. H. Dunning, J. H. Robert, *J. Chem. Phys.* **1992**, *96*, 6796–6806.
- [53] A. P. Kirk, E. W. David, T. H. Dunning, *J. Chem. Phys.* **1994**, *100*, 7410–7415.
- [54] H. Xue, H. Gao, B. Twamley, J. M. Shreeve, *Chem. Mater.* **2007**, *19*, 1731–1739.
- [55] a) ICT-Thermodynamic Code, v. 1.0, Fraunhofer Institut für Chemische Technologie (ICT), Pfinztal, Germany, **1988–2000**; b) R. Webb, M. van Rooijen, *Proceedings of the 29th International Pyrotechnics Seminar*, **2002**, pp. 823–828; c) H. Bathelt, F. Volk, *27<sup>th</sup> International Annual Conference of ICT*, **1996**, *92*, 1–16.
- [56] Y. N. Matyushin, T. S. Kon'kova, A. B. Vorob'ev, Y. A. Lebedev, *36th International Annual Conference of ICT* **2005**, *92/1–92/9*.
- [57] a) T. M. Klapötke, J. Stierstorfer, *Chem. Sus. Chem.*, submitted; b) T. M. Klapötke, J. Stierstorfer, *New Trends in Research of Energetic Materials*, Proceedings of the 11th Seminar, Pardubice, Czech Republic, **2008**, *2*, 810–831.
- [58] N. Wingborg, N. V. Latypov, *Propellants Explos. Pyrotech.* **2003**, *28*, 314–318.
- [59] H. R. Blomquist, US 6004410, **1999**.

Received: October 8, 2008

Published Online: January 28, 2009